BREAST CANCER DETECTION BY MAGNETO-THERMAL MODELING OF BIOLOGICAL TISSUES

by

Sepideh Rahmatinia

APPROVED BY SUPERVISORY COMMITTEE:

Dr. Babak Fahimi, Chair

Dr. Bilal Akin

Dr. Poras T. Balsara

This thesis is dedicated to my family

BREAST CANCER DETECTION BY MAGNETO-THERMAL MODELING OF BIOLOGICAL TISSUES

by

SEPIDEH RAHMATINIA, BS

THESIS

Presented to the Faculty of

The University of Texas at Dallas

in Partial Fulfillment

of the Requirements

for the Degree of

MASTER OF SCIENCE IN

ELECTRICAL ENGINEERING

THE UNIVERSITY OF TEXAS AT DALLAS

December 2016

ACKNOWLEDGMENTS

This thesis becomes a reality with the kind support and help of many individuals. I would like to extend my sincere thanks to all of them. Foremost, I would like to express the deepest appreciation to my advisor, Professor Babak Fahimi, who has the attitude and the substance of a genius. The completion of this undertaking could not have been possible without his guidance and persistent help.

I would like to thank my committee members, Professor Bilal Akin and Professor Poras T. Balsara for their constructive comments, suggestion and critiquing.

My thanks and appreciations also go to my colleagues and people who have willingly helped me with their abilities.

November 2016

BREAST CANCER DETECTION BY MAGNETO-THERMAL MODELING

OF BIOLOGICAL TISSUES

Publication No. _____

Sepideh Rahmatinia, MS
The University of Texas at Dallas, 2016

Supervising Professor: Dr. Babak Fahimi

Breast cancer has adversely influenced women's lives for many years. Yet, the current cancer detection methods come with disadvantages such as lack of reliability, health concerns, and high operational costs. This research contributes to the theory and practice of cancer detection technique by introducing a novel method which combines thermal and electromagnetic responses of human body to radio frequency excitation. Using several simulation studies, It is demonstrated how the differences in magneto-thermal properties of malignant and healthy breast tissues can be exploit to pinpoint the size and location of a cancerous tumor.

TABLE OF CONTENTS

LIST OF FIGURES

LIST OF TABLES

CHAPTER 1

INTRODUCTION

1.1 Overview of Breast Cancer Detection Methods

Breast cancer has adversely influenced women's lives for many years. This disease has been noticed in almost every period of recorded history. People in ancient Greece and Egypt were the first groups that discovered this disease. According to American Cancer Society, breast cancer is the most common type of cancer in women, affecting approximately 200,000 cases every year in the United States. This disease is also the second cause of death in women diagnosed with cancer. Nevertheless, breast cancer can be treated efficiently if it is detected in the early stages. In fact, research has shown that the survival likelihood of patients is highly related to the progress stage of the disease. As a result, an effective and precise method for detecting breast cancer is crucial.

In the last few decades, a variety of techniques have been developed to detect breast cancer in its early stages. These techniques are different regarding their precision to detect cancer, cost and difficulty of operation, and required equipments. The ideal method for breast cancer detection should have at least three important characteristics. First, the method should have Minimum health risk and discomfort for patients.Often, methods that are used are not without side effects and sometimes might cause serious health issues for the patients, especially the intrusive methods. Second, it is important that the operation is affordable. Many of these techniques are very expensive and usually are not covered by most of insurance companies. Finally, the method should be able to detect cancer with good precision and in the early stages of disease. Controlling the spread of the cancerous tissue becomes increasingly difficult in the late stages of the cancer disease.

Today's common methods for breast cancer detection are X-ray, mammography, ultra sound, MRI and thermography. Each of these methods have their own strengths and weaknesses. To understand how the approach that is proposed in this dissertation is compared to current commercial breast cancer detection techniques, an overview of these methods are provides below, and their advantages and disadvantages are discussed.In general, detection techniques can be classified in two broad categories. First, Electromagnetic technique such as mammography, ultrasound and MRI, which use electromagnetic fields and create images of different body parts. The second category is thermography and thermal imaging methods such as OCT and EIT. These methods use the variations in body temperature to create thermo-graphical high quality images.

1.1.1 Electromagnetic techniques for breast cancer detection

Mammography

Mammography techniques can be used to detect small breast tumors in early stages. This technique uses ionizing radiation to create images. An specialist then examines these images to find and locate malignant breast tissue. According to Food and Drug Administration (FDA) mammography can detect 85% of breast cancers.

During the procedure, breast is placed and compressed between two mammography units. Compression helps creating higher quality images by reducing the thickness of breast and decreasing scatter radiation dose. As shown in figure1.1 , a camera unit is located on top of the breast to capture the image.

Mammography is a low cost technique and it is one of the most effective tools for early detection of cancer. In the last two decades, this diagnostic technique has significantly reduced the mortality rate related to breast cancer. In 2005, mammography contributed to 25% reduction in death rate from breast cancer. This has happened because of the widespread usage of screening mammography. Despite mentioned benefits, there are potential harms

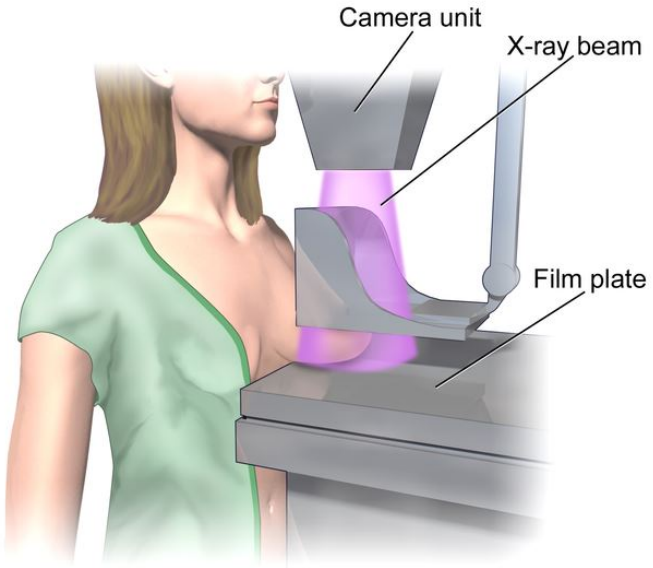

Figure 1.1. Mammography illustration

and shortcomings associated with mammography, such as subsequenttreatment, radiation and surgery. Somtimes these side effects can be as harmful as untreated cancer [13]. Moreover, it is uncomfortable for many patients to go through the examination on a regular basis. Furthermore, there is a 15% chance of missing an actual tumor which can be detected by physical diagnosis [18]. Finally, it is difficult to detect dense breast with mammography. This is due to the fact that dense breast appears white in mammography which hinders the detection of malignant tissues. Figure 1.2, [6] shows a comparison between fatty and dense breast. As illustrated, it is difficult to pinpoint any cancerous tumor in dense breast. Therefor, false negative results will appear and the cancer remains undetected.

Ultrasound

Ultrasound imaging uses high frequency sound waves. This technique can distinguish different parts of tissue such as skin, gland, muscle and fat based on reflection intensity of ultrasound waves. Ultrasound imaging is radiation free and low cost. Oftentimes, ultrasound is used in combination with other cancer detection methods such as biopsy.

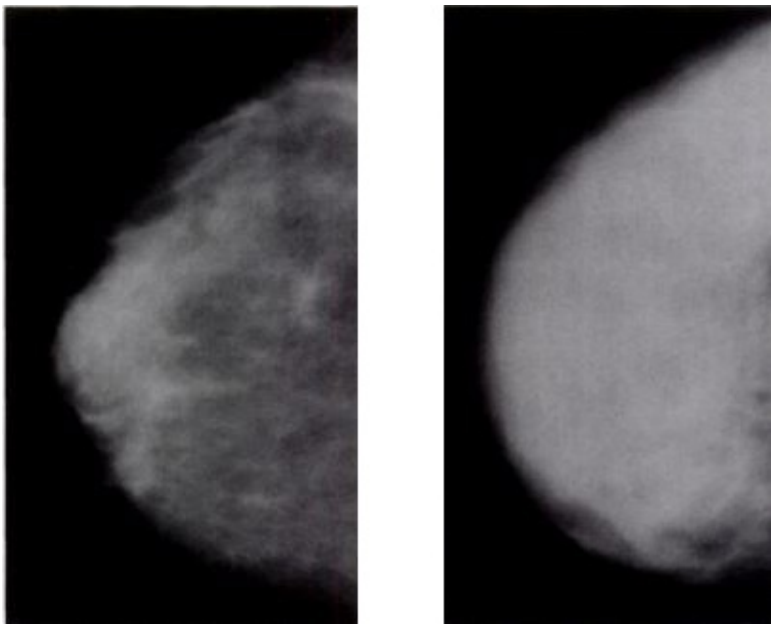

(a) Fatty Breast (b) Dense Breast

Figure 1.2. Breasts Imaging using Mammography

One of the most important drawbacks of ultrasound is its lack of ability to distinguish between cancerous tissue and breast fat. This is due to the fact that fat and cancerous breast have similar acoustic characteristics which can not be identified with ultrasound imaging. Furthermore, this method is implemented by hand-held devices which might increase the error component in results. Ultrasound mainly remains a tool for distinguishing cysts from solid tumors and for guiding biopsy procedures.

Magnetic Resonance Imaging(MRI)

MRI techniques create images using magnetic fields and radio waves. In this method, the nuclei of atoms such as hydrogen are resonated in a strong magnetic field which causes them to radiate radio frequency waves that can be detected with an antenna. The antenna is located close to body. MRI has application in a wide variety of situations such as biomedical research, diagnostic medicine, and even non-living objects.

Previous studies[14][27] show that MRI is capable of detecting many cancers that were undetectable by mammogram or ultrasound. This method has shown considerable progress in detection power. The color-enhanced MRI has been shown to be an enormous aid in detection of cancerous tissues (see Figure 1.3) [19]. Despite its effectiveness and popularity, this method has some drawbacks. For example, low specificity in MRI may cause high rate of false positive results compared to other methods[[17]. Moreover, its high cost of operation can limit MRI's application for regular check-ups.

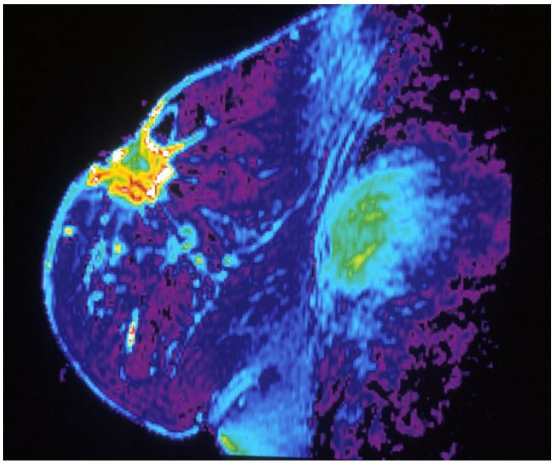

Figure 1.3. Color-enhanced MRI of a breast

Microwave Thermography

Microwave thermography technique is based on emitted radiation from the body in microwave region. It uses antenna to measure the interaction of electromagnetic waves and breast tissues. The antenna is placed close to the tissue and is directed towards body surface. This method can detect a cancer by comparing dielectric properties of normal and abnormal tissue.

In order to have maximum percentage of true positive and true negative rates, microwave and infrared themrography need to be combined [4].

1.1.2 Thermography and thermal Imaging

Optical Coherence Tomography(OCT)

Optical Coherence Tomography(OCT) is a non-invasive medical imaging technique which is used to obtain surface images of objects. OCT creates images based on light and uses low-coherence interferometry. Three dimensional images of body parts can be constructed by applying interferometry of near-infrared light wave.

Instant and direct imaging of tissue are two key advantages of OCT. Moreover, there is no harm for patients since there is no ionizing radiation. However, OCT does not provide preferred length of penetration which can results in low accuracy of results and high false positive rates.

Electrical Impedance Tomography(EIT)

EIT is a non-invasive technique to create high-quality images. In this method, electrodes are either directed towards the skin or connected to a conductive object which has been attached to the skin. A small AC current then is applied to the couple of electrodes and the remaining electrodes calculate the voltage. Based on the measured voltage and collected data, an inverse problem is solved and an image of the breast tissue is created.

Thermoacoustic Imaging

This method combines microwave and ultrasound imaging elements for detection. Figure 1.4 [15] illustrates the process of this method. First, tissue is irradiated with microwave radiation. Absorbed energy from microwave radiation is converted to heat that marginally increases tissue temperature. Temperature elevation causes the tissue to expand and produce acoustic waves. These acoustic waves are observed by transducer array and used to generate images.

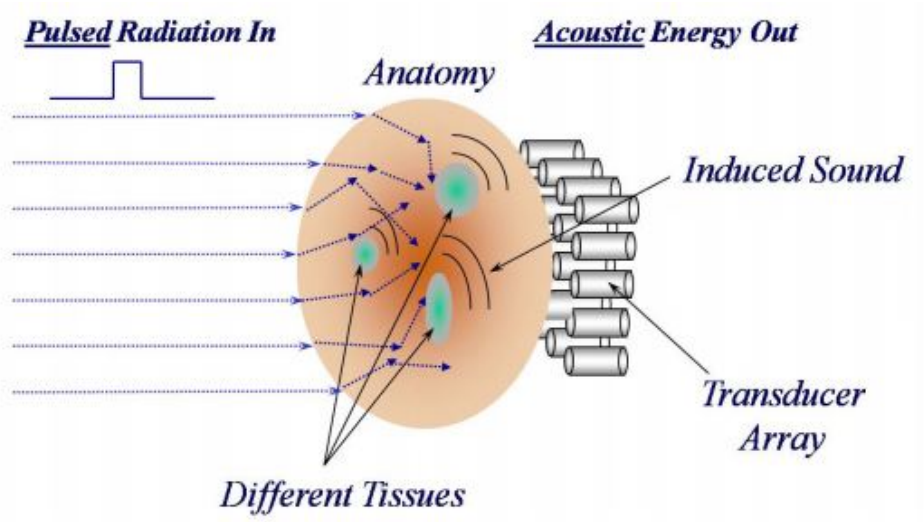

Figure 1.4. Thermoacoustic Imaging

1.2 Research motivation and goals

Breast cancer has had an adverse effect on women's lives in the world. Yet, there is not a low-cost, precise technique that can be used as a monitoring tool to detect the cancer in its early stage. The main goal of this research is to come up with a effective and novel conceptual technique that can be used to design and develop an efficient, practical and possibly wearable device for breast cancer detection.

The method which is introduced in this research combines two major approaches to breast cancer detection,namely, electromagnetic and thermal approach. The reason for combining these two approaches is to obtain maximum benefit of each method while reducing the health risk for patients. The proposed method uses the distribution and variation of the temperature on breast surface in order to estimate the location and size of a malignant breast tissue (a cancerous tumor). First, breast tissue is excited with a radio frequency antenna and electromagnetic analysis is conducted. Next, bioheat equation is solved in order to estimate the distribution of surface temperature. Simulation results show that both

the temperature and specific absorption rate (SAR) increase as the tumor becomes larger or closer to the surface.

1.3 Thesis Outline

The different chapters of this thesis is outlined below:

- Chapter 1: In this chapter, existing breast cancer detection methods are reviewed and their procedures, benefits and drawbacks are discussed. The thesis objective is defined..
- Chapter 2: Fundamental electromagnetic and thermal behavior of biological tissue are investigated. Important factors for electromagnetic and thermal analysis are mentioned. A cubic tissue model is simulated to measure temperature elevation as a result of radio frequency excitation.
- Chapter 3: A normal and a malignant breast model are simulated. The rate of absorbed energy as a function of various frequency ranges is analyzed. Moreover, thermal and electromagnetic analysis problem of breast cancer detection is studied.
- Chapter 4: Two methods of breast cancer detection are combined to provide a new technique. Detection strategy and simulation results are presented in this chapter.
- Chapter 5: The key insights of proposed technique are discussed. Future research directions are proposed.

CHAPTER 2

ELECTROMAGNETIC AND THERMAL BEHAVIOR OF BIOLOGICAL TISSUE

In the first part of this chapter, fundamentals of electromagnetic behavior of biological tissues were explained. One of the important factors that defines electromagnetic behavior is dielectric parameters and their changes with respect to frequency. In the first part of this chapter, different types of dielectric parameters such as conductivity and permittivity are reviewed and their variations to frequency are studied. In the second part of the chapter, analysis of thermal and bio-heat equations are performed. This analysis specifies how much the temperature changes due to the biological elements. In the last part of this chapter, a finite element simulation is performed to characterize the electromagnetic and thermal behavior of biological tissues.

2.1 EM behavior

The emission or transmission of energy by waves through a medium is called radiation. Electromagnetic waves influence biological tissues through radiation waves. Combination of electric fields and magnetic fields form electromagnetic radiations.

There are two main types of radiations; ionizing radiations, and non-ionizing radiations. The ionizing radiation has a high level of energy which can break into medium and ionize its atoms. The non-ionizing radiation has a lower amount of kinetic energy compared to ionizing one and it is capable of vibrating or rotating molecules and atoms. Both types of radiations influence the dielectric parameters of tissue or medium. Therefore, it is essential

to understand dielectric properties of biological tissues and investigate their changes with respect to radiation and frequency variations.

2.1.1 Dielectric properties of biological tissue

The electrical properties to be reviewed include conductivity and permittivity relative to free space. The dielectric properties of materials are measured through their complex permittivity ($\hat{\epsilon}$).

$$\hat{\epsilon} = \epsilon' - j\epsilon" \tag{2.1}$$

Equation(2.1) shows the relation between complex permittivity($\hat{\epsilon}$) and its two component relative permittivity (ϵ') and ϵ" that is related to the loss of energy in the medium[9]. Furthermore, relative permittivity (ϵ') is related to the medium conductivity through the following relationship.

$$\epsilon' = \frac{\sigma}{\epsilon_0} \tag{2.2}$$

Equation (2.2) depicts the relation of ϵ" and conductivity where $\epsilon_0 = 8.85 * 10^{-12}$ is permittivity of free space. The interaction of electromagnetic radiation with atoms causes variations in dielectric properties of biological tissue [9].

Dielectric properties depends on many factors such as age, tissue material, frequency and even range of frequency. Some of these factors will be explored in this section.

Figure 2.1 depicts the brain conductivity and permittivity of 10-day-old and 70s-day-old rats. The difference between conductivities of these two type of rats is related to the water content in their bodies. As rats become older, the amount of body water decreases. As a result, permittivity and conductivity are lower in older rats. It should be noted that conductivity and permittivity are respectively decreasing and increasing in frequency for both types of rats.

Relative permittivity of biological tissues decrease with frequency in three dispersion levels which are called α-dispersion, β-dispersion and γ-dispersion. The α-dispersion is

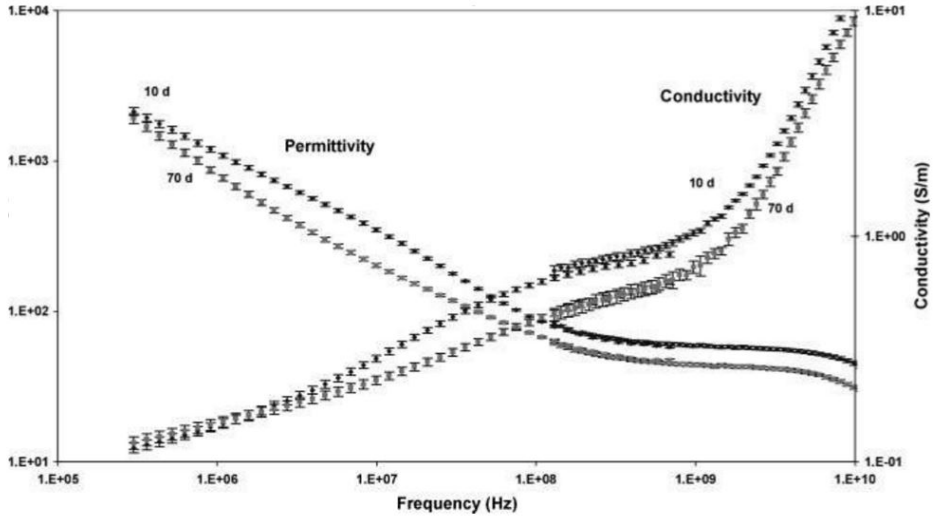

Figure 2.1. Dielectric properties of rat's brain[8]

related to the surface ionic conduction effects at membrane boundaries and polarizations of electrical layers. The β-dispersion is associated with capacitance shorting-out of membrane resistance and rotational relaxations of bio-macromolecules. Finlay, the γ-dispersion comes from bulk water in tissue. Figure 2.2 illustrated these three dispersion levels in an idealized plot of frequency versus relative permittivity of biological tissue[22].

In Figure 2.3, the change of relative permittivity with respect to range of frequency is illustrated. The relative permittivity decreases for lower frequency because the cellular membranes affect tissue impedance at lower frequency. A decline occurs above 100 MHz in the curve is due to the γ-dispersion. In other word, the water in biological tissue changes with frequency. As mentioned, relative permittivity also depends on water content in biological tissue. Figure 2.4 shows that the amount of water content in fat has direct relationship with relative permittivity. Same conclusion can be true for conductivity. In figure 2.5 conductivity is depicted as a function of water content of the tissue. [25].

There are different types of water in human body tissues (e.g, normal water and bound

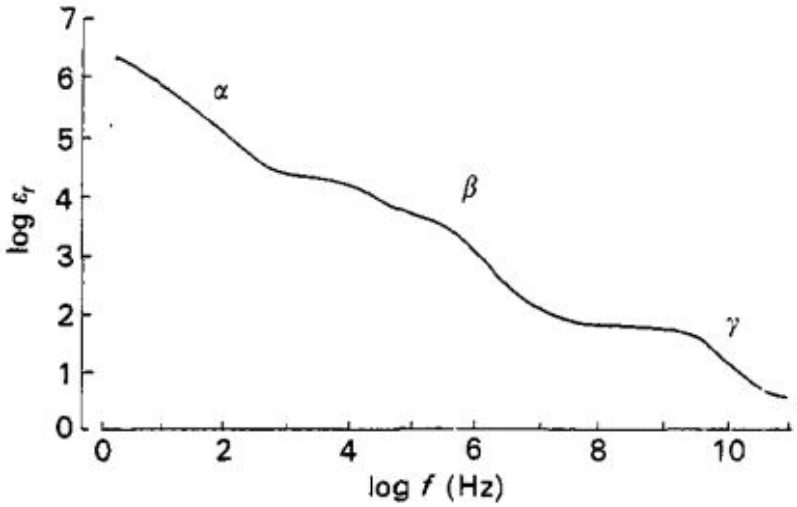

Figure 2.2. Idealized plot of frequency vs relative permittivity in typical biological tissue[22]

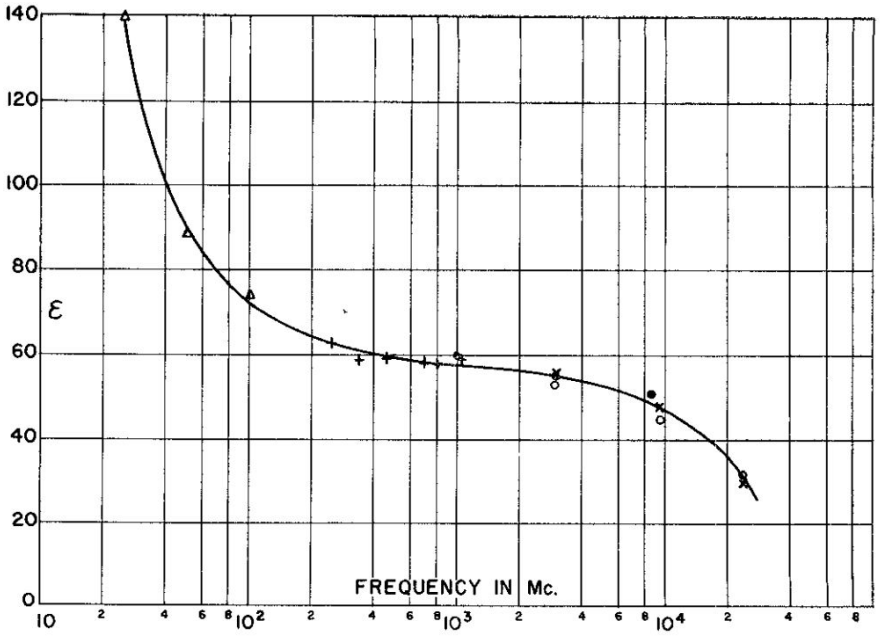

Figure 2.3. Relative permittivity of blood vs frequency [25]

water). Each type of body water has its own dielectric characteristic [25]. Measurements in [7] and [11] show that malignant tissue have significantly higher water content than normal

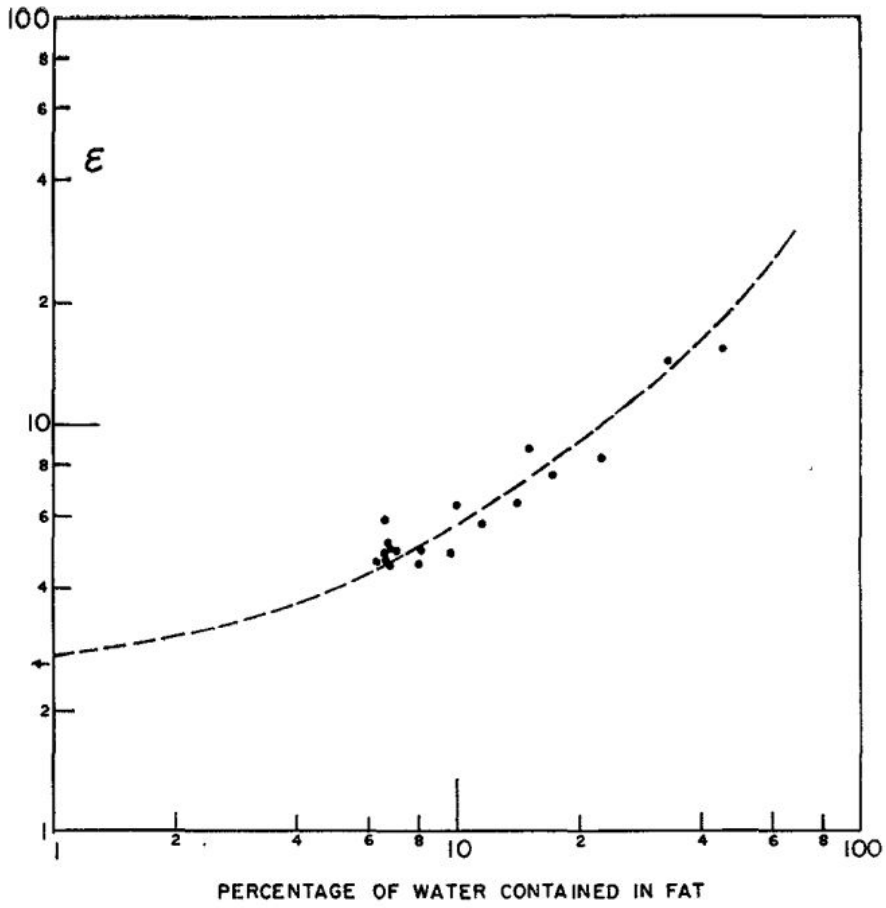

Figure 2.4. Relative permittivity of fatty tissue as function of its water content. Frequency, 900 MHz. [25]

tissue, which will be discussed in more detail in chapter three. For instance liver hepatoma tissue has 15% more water than normal liver tissue[10].

All of the mentioned characteristic of dielectric properties have provided an important contribution in oncology science. Most of the tumors can be detected by tracking dielectric properties variation in tissue. Hence, it is necessary to understand dielectric properties of body tissue to analyze and detect biological tumors.

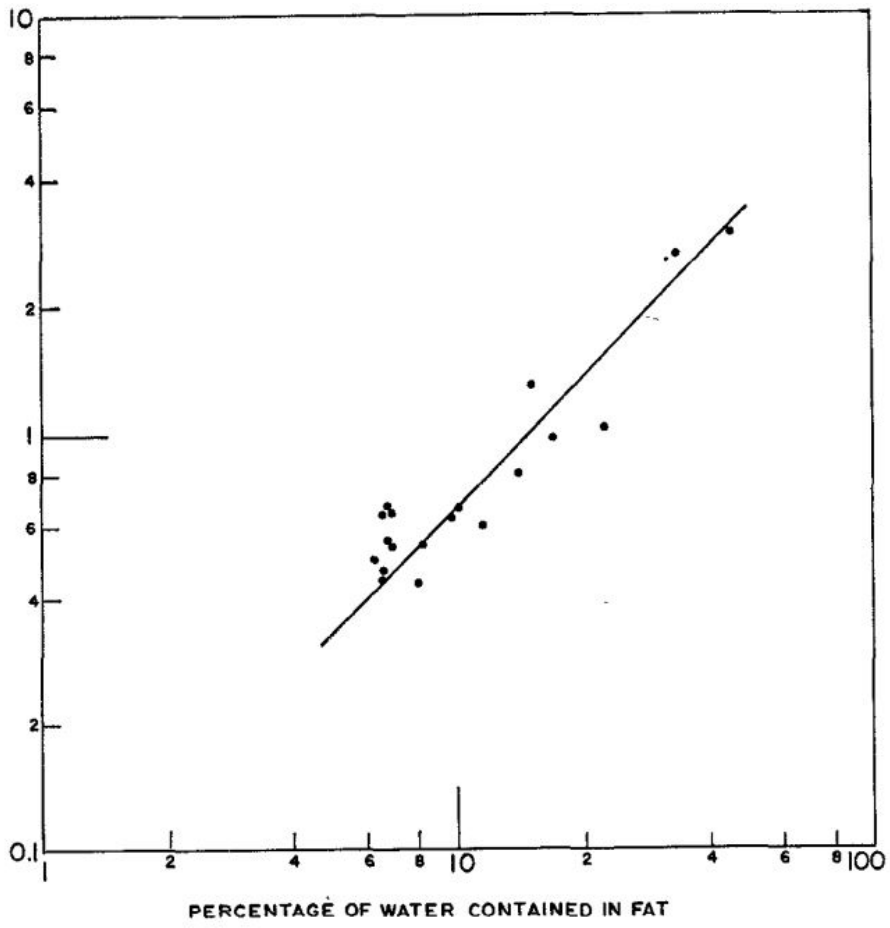

Figure 2.5. Conductivity of fatty tissue as function of its water content. [25]

2.1.2 Specific Absorption rate (SAR)

In order to establish human safety exposure to high frequency, a standard rate has been established which is called specific absorption rate (SAR). SAR is a measure of absorbed energy by human tissue when it is exposed to radio frequency electromagnetic field. SAR calculates exposure to fields in range of 100 kHz to 10 GHz. The SI unit for SAR is W/Kg. For protecting human body from adverse thermal effect of high frequency radiation, some limits have been considered. For instance in the Federal Communications Commission (FCC) of the U.S, a general value of 4 W/Kg averaged over the whole body is considered. Furthermore, for the localized near field exposure application, a value of 1.6 W/Kg averaged over 10

g of tissue is established. [12]. In the Council of the European Union, a value of 2.0 W/Kg over 10 g of tissue is established [21] for maximum SAR exposure. All of mentioned value will cause a safe exposure in terms of electric and magnetic fields.

SAR measurement

To calculate SAR, it is essential to know the RMS value of incident electric field entering the tissue. SAR is defined as,

$$SAR = \frac{1}{V} \int \frac{\sigma(r)) \left|E(r))\right|^2}{\rho(r)} dr \tag{2.3}$$

Where ρ and σ are density and conductivity of sample tissue and V is the volume of sample tissue. Temperature elevation in body can be calculated base on the value of SAR, which will be discussed in the next section.

2.2 Thermal behavior of biological tissue

Temperature distribution inside an exposed human body can be calculated using bio-heat equation. To understand bio-heat equation, heat equation is reviewed first.

Heat Equation

Heat equation is a parabolic differential equation that calculates distribution of heat over a specified region in a matter of time. For instance, in a metal rod with non-uniform temperature distribution, heat energy moves from higher temperature part to lower temperature part. Three principle rules are applied to explain the thermal distribution:

1. Thermal energy in a medium with non-uniform distribution is calculated from,

$$Heat\ energy = cmT \tag{2.4}$$

   Where m is the medium mass, and c is the medium's specific heat, which is the required energy to increase temperature of body by one degree.

2. Base on Fourier's law of heat transfer, temperature is transfered from higher temperature part to lower temperature part. Consequently, rate of heat transfer is relative to negative temperature gradient,

$$\frac{Rate\ of\ heat\ transfer}{area} = -K\frac{\partial T}{\partial t} \tag{2.5}$$

3. Conservation of energy implies that the change of heat energy is equal to the difference of heat in and out. In another word, by energy conservation law in an insulated medium, energy does not vanish, just transfer from one form to another.

By rearranging three principles above, the general form of heat equation is obtained,

$$\rho c_p \frac{\partial T}{\partial t} = K\nabla^2 T + Q \tag{2.6}$$

In Equation(2.6), T is the temperature at any point in space at any time, ρ is Mass density, c_p is specific heat capacity, K is the thermal conductivity, and Q is the heat generated per unit volume.

Bioheat Equation

Heat transfer in biological tissues is described by a more complex form of heat equation. It is complicated due to the existence of many metabolism factors in human body which make the measurement of heat transfer a challenging task. First, Heat transfer in tissue includes radiation, convection and radiation and It is challenging to decouple these effects. Second, tissue structure of each sample is unique. Finally, Thermal properties of tissue depend on the environment temperature and water content [5, 26].

Over several years, many mathematical models have been developed to overcome these complexities. These models have been widely used in medical application such as cancer treatment and laser surgery. The most popular bioheat model was proposed by Pennes in 1984. This model has been applied to a wide range of heat transfer problems. Several

other bioheat models of human body were built on Pennes's model in order to extend its application and overcome its drawbacks. Pennes and other bioheat models will be explained briefly in the following sections.

Pennes Equation

There are two main approaches for bioheat modeling of body; continuum vessels and discrete vessels. In the continuum approach, temperature variation of all blood vessels is represented with one global parameter. On the other hand, thermal effects of each blood vessel is modeled separately in discrete vascular approach[23]. The most common continuum approach is Pennes equation. In Pennes model, the effect of blood flow on body temperature is captured through an isotropic heat source or sink. This heat source in human body is proportional to the blood flow and temperature difference of body core and local tissue. Based on these assumption, Pennes equation is formed [3],

$$\rho_{ti} C_{ti} \frac{\partial T_{ti}}{\partial t} = k_{ti} \nabla^2 T_{ti} + \rho_{bl} C_{bl} W_{bl} (T_{bl} - T_{ti}) + Q_m \tag{2.7}$$

Where ρ_{ti}, C_{ti}, T_{ti} and k_{ti} are density, specific heat, temperature and thermal conductivity of tissue.Moreover, T_{bl} is the blood temperature and Q_m is the metabolic heat generation. Finally, ρ_{bl}, C_{bl}, W_{bl} are density, specific heat and perfusion rate of blood. This equation represents how heat is transfered in biological tissues. It also describes heat generation and transfer based on blood perfusion in body. In other word, Pennes considers blood regulation of body to measure the temperature.

There are several works that extend and enhance Pennes model. Wulf and Klingeer (1974) added the local mean blood velocity in their model. Chen-Holmes(1980) proposed that larger vessel be modeled separately from smaller vessels and tissue. Despite all of the enhancements and modification, mentioned models are hard to implement and test. In this thesis, the base Pennes equation has been used to model heat transfer in human breast .

2.3 Simulation Analysis

A finite element simulation is performed in ANSYS electromagnetic and mechanical platform to measure SAR and temperature elevation in human body. The simulation flowchart has been illustrated below,Figure 2.6.

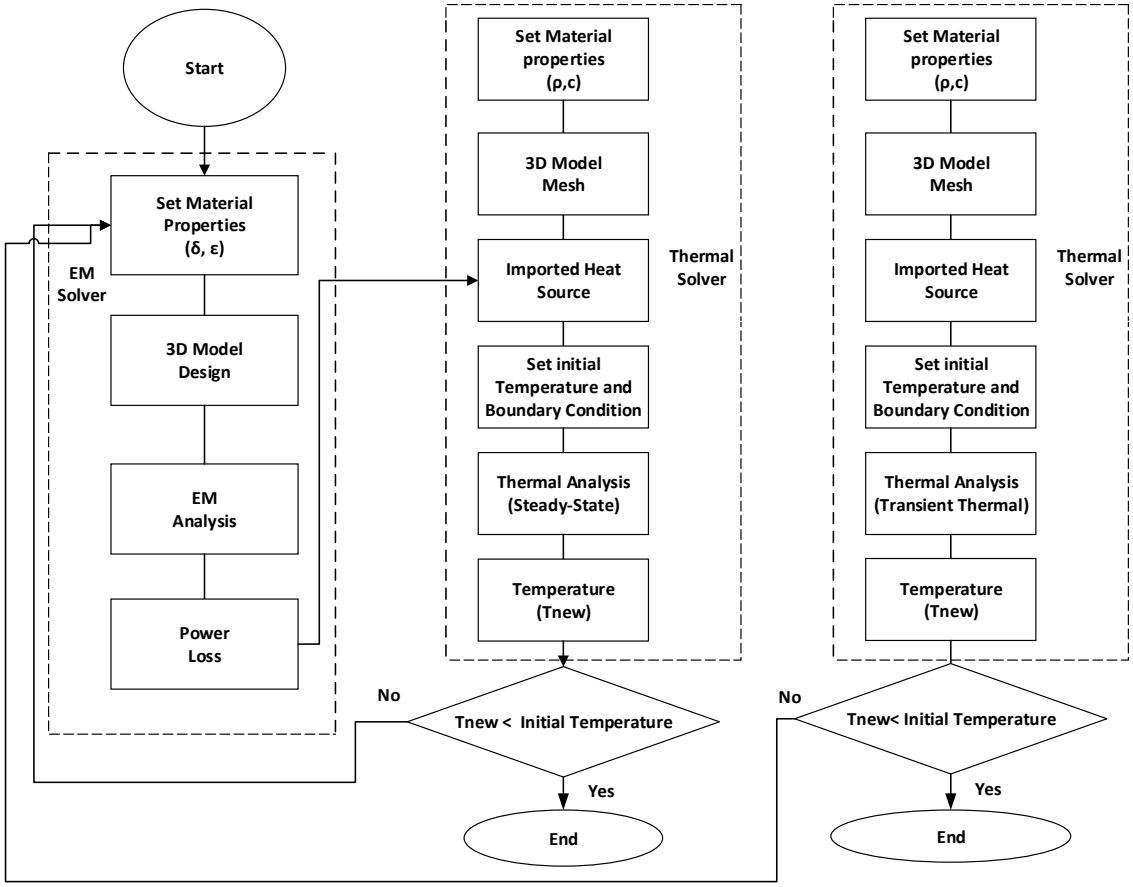

Figure 2.6. Simulation Flowchart

This simulation has three main parts:

1. The generated heat due to radio frequency radiation is calculated in electromagnetic analysis. First, frequency-dependent materials are modeled and their parameters are

defined. Second, the geometry of the model is drawn and mesh partitioning is designed.Third, finite element analysis is performed to measure power loss and generated heat. A cubic form of human body is modeled for this simulation. This geometry consists of skin, fat, muscle and spinal chord, depicted in Figure 2.7.

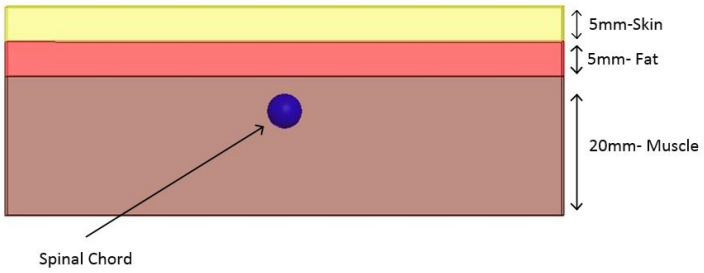

Figure 2.7. model

The materials used in the model in Figure 2.7 are frequency dependent. This implies that conductivity and permittivity of skin, fat, muscle and spinal chord vary with respect to frequency. Table2.1 shows the dielectric parameters which has been for the simulation of this model.

Table 2.1. Dielectric Parameters of Simulated Model

Frequency (GHz)	**Mussle**		**Fat**		**Spinal**	
	ϵ	σ (S/m)	ϵ	σ (S/m)	ϵ	σ (S/m)
0.01	160.0	0.64	29.58	0.05	155.1	0.22
0.02	107.2	0.67	20.71	0.05	97.62	0.25
0.05	76.45	0.70	14.45	0.06	60.84	0.29
0.1	66.19	0.73	12.70	0.06	47.26	0.33
0.2	60.87	0.76	11.90	0.07	39.71	0.38
0.5	57.32	0.84	11.54	0.08	34.45	0.47
1	55.74	1.00	11.29	0.11	32.25	0.59
2	54.17	1.50	10.96	0.21	30.63	0.91
4	51.52	3.15	10.36	0.50	28.74	1.83
6	48.70	5.45	9.80	0.87	27.05	3.07

In order to excite the tissue, a wire dipole antenna (Figure 2.8) is placed on top of the cubic model. Various dimensions of antenna are summarized in table 2.2.The solution frequency of this antenna is equal to 915 MHz. Figure 2.9 illustrates antenna's reflected power as a function of frequency. It can be observed that the maximum power is radiated from the antenna at 915 MHz (resonance frequency). This shows that antenna is working well at desired frequency.

Figure 2.8. dipole antenna

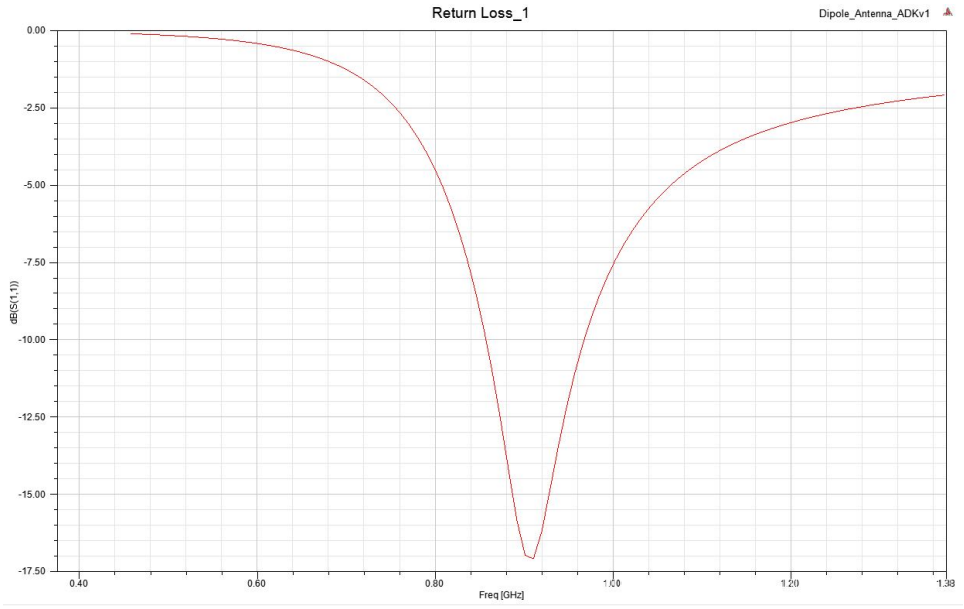

Figure 2.9. Dipole antenna return loss

Table 2.2. Dipole Antenna Size at 915 MHz in cm

Dipole Length	Dipole Radius	Feed Gap
14.75	0.246	0.246

The generated heat and specific absorption rate results will be shown in results section of this chapter.

2. In steady-state thermal analysis physical properties are specified as shown in table 2.3. These properties determine how much the temperature rises due to the heat generated. In order to see the temperature variation with higher precision, accurate mesh elements are assigned in the cubic geometry in thermal solver, Figure 2.10. Heat and bio-heat equations are solved in this section by defining boundary conditions. If the final temperature is lower than the initial temperature then the whole loop will be repeated to debug the problem.

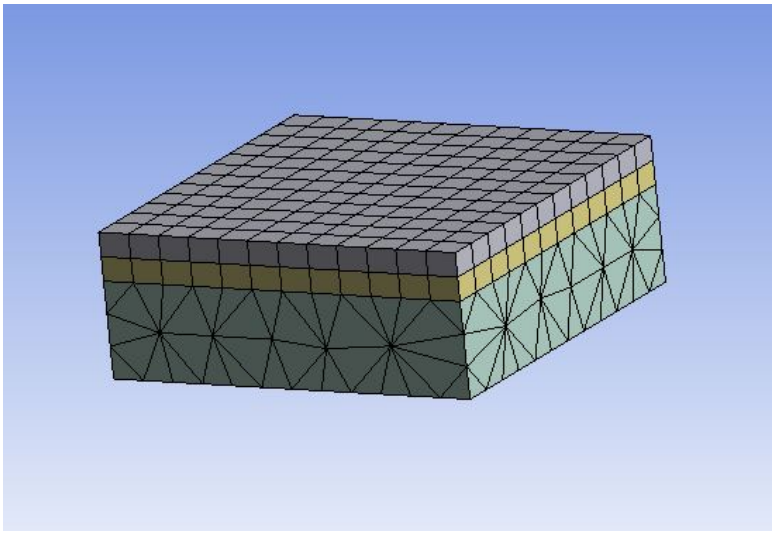

Figure 2.10. Simulation Mesh

Table 2.3. Thermal simulation parameters

Tissue	Density ($\frac{Kg}{m^3}$)	Isotropic Thermal Conductivity($\frac{W}{mC}$)	Specific Heat ($\frac{J}{KgC}$)
Skin	1109	0.37	3391
Fat	911	0.21	2348
Muscle	1090	0.49	3421
Spinal Chord	1075	0.51	3630

3. Transient thermal simulation follows basically the same process as the steady-state thermal simulation. The most important difference is that applied load(Imported heat) in transient analysis is time dependent.

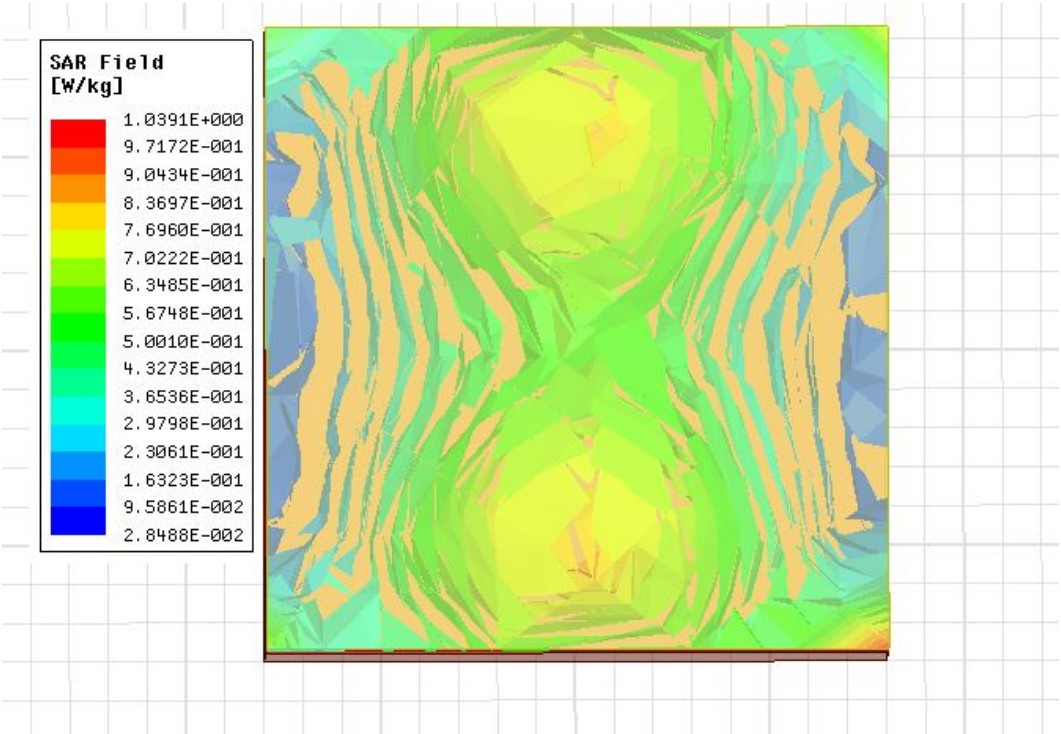

Figure 2.11. SAR Inside of The Skin

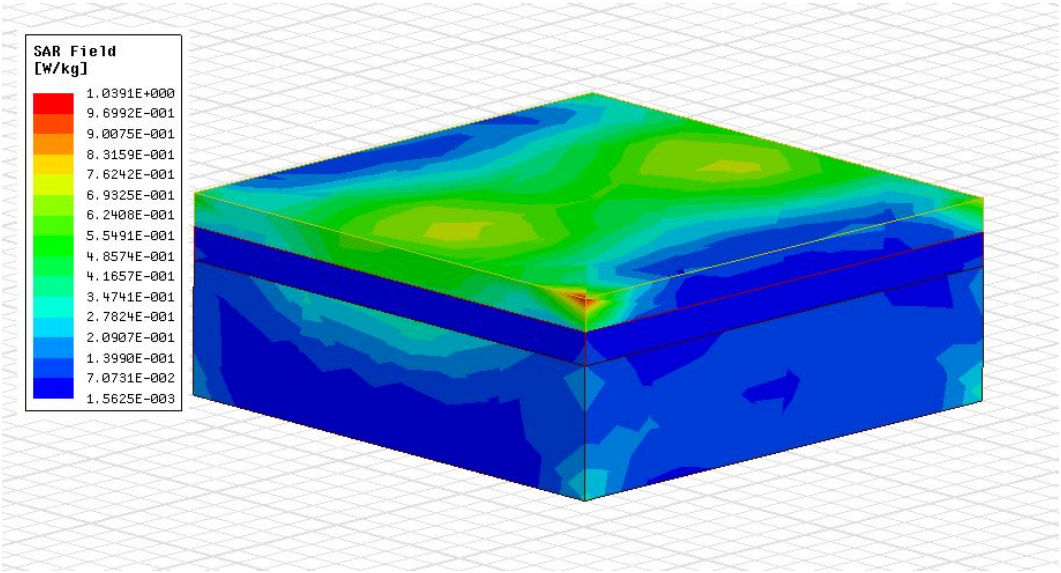

Figure 2.12. SAR on Tissue Surface

2.3.1 Electromagnetic Analysis Results

After finishing electromagnetic simulation the SAR of the skin has been calculated. Figure2.11 shows how much energy has been absorbed through antenna radiation inside the skin, the value of SAR on the right and left side is lower due to antenna direction. Figure 2.12 depicts SAR on the surface of the whole tissue, the SAR on skin's surface is higher than fat and muscle surface, because the antenna is radiating directly to the skin surface. As a result, more energy is absorbed. SAR calculation method in Ansys will be explained in more details in chapter 3.

2.3.2 Thermal Analysis results

In steady-state thermal (SST) analysis, temperature distribution has the same pattern as SAR. This shows that the generated heat has been imported accurately from electromagnetic solver to thermal. Figure 2.13 illustrates temperature distribution on surface of the tissue and Figure 2.14 depicts temperature distribution on surface after applying bio-heat equation. Temperature has been decreased after considering bio-heat equation due to the

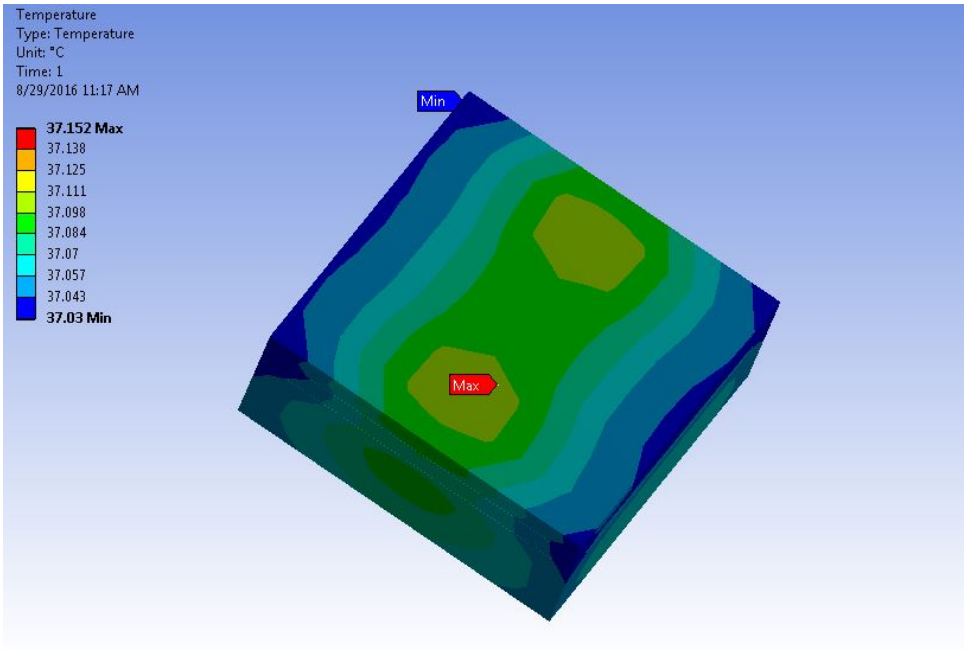

Figure 2.13. Temperature distribution on tissue in SST analysis

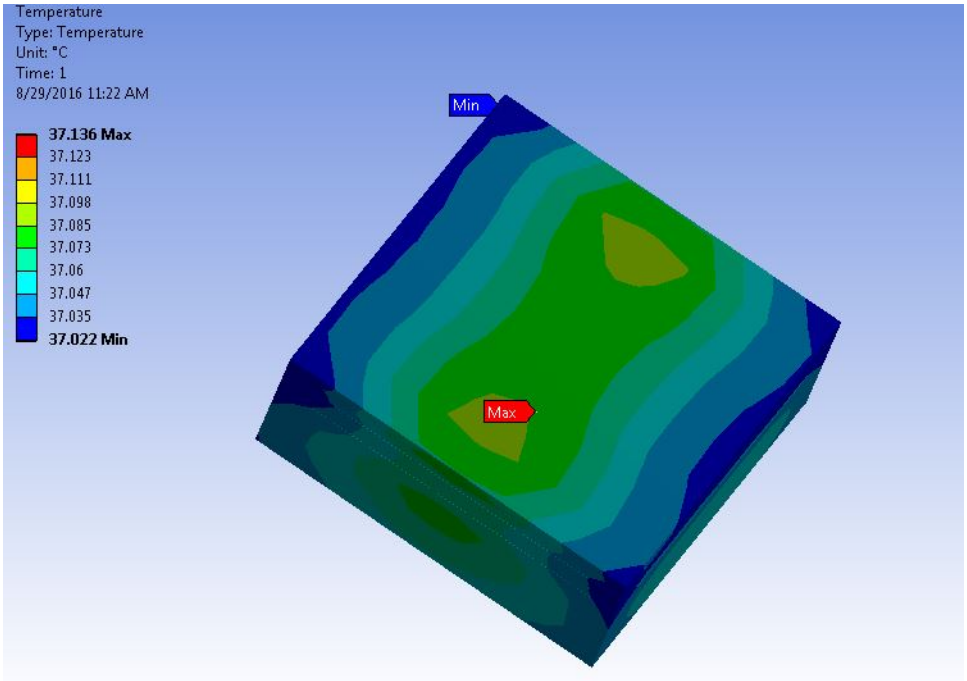

Figure 2.14. Temperature distribution on tissue with bioheat equation

blood perfusion concept. Blood perfusion acts as regulatory system and help the body to stay cool.

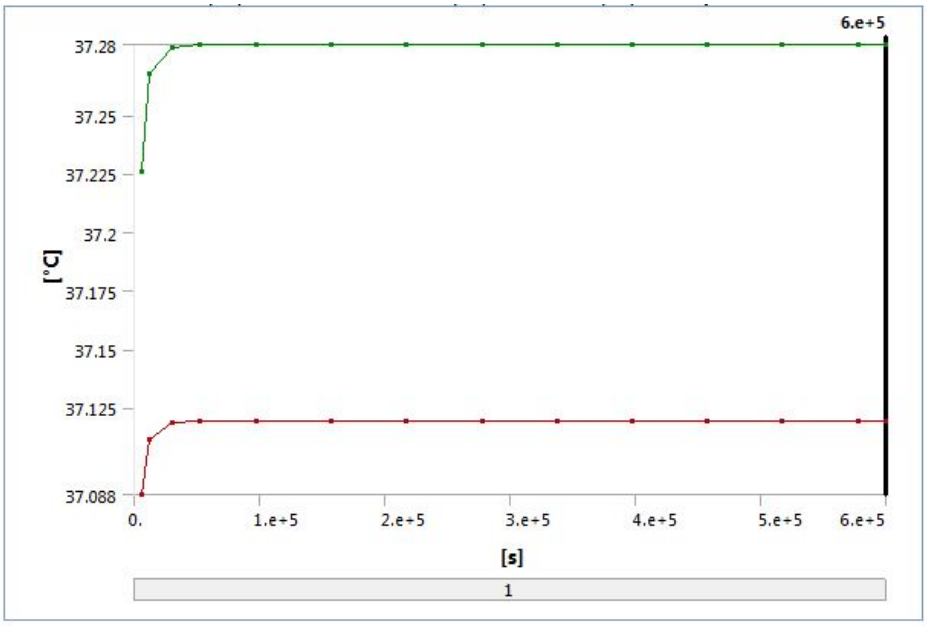

Figure 2.15. Temperature distribution on Tissue with bio-heat equation

In transient thermal analysis, global minimum and maximum temperature are measured. Minimum temperature occurs on fat and maximum occurs on muscle. This happens as a results of their thermal properties. Figure 2.15 shows the transient thermal temperature in 600000 second. The green line is global maximum and the red is global minimum.

2.4 summary

In this chapter the electromagnetic and thermal behavior of biological tissue is investigated. Significance factors such as dielectric and thermal properties are explained. One of the important factors in terms of energy absorption in biological tissue is dielectric properties which should be carefully analyzed and considered in simulations and experiments. Moreover in thermal analysis of human tissue, bioheat equation needs to be involved in order to have the accurate temperature.

A finite element simulation is performed to investigate absorbed energy value and temperature elevation. As the value of SAR increases the temperature will increase as well. The results would be useful for reviewing the electromagnetic exposures.

CHAPTER 3

NUMERICAL ANALYSIS FOR BREAST CANCER SIMULATION

Electromagnetic analysis and simulation of breast is an essential step for development of knowledge about breast cancer. It also provides insight about malignant and normal breast tissues. In this chapter, a finite element (FEA) analysis of malignant and normal breast tissue is established. Furthermore, tissue parameters and details of the design are demonstrated.

3.1 Breast Anatomy

In the development of an altenrnative method for breast cancer detection, it is essential and important to have a basic knowledge about the anatomy of breast. A breast anatomy is shown in Figure 3.1. It depicts skin gland that lies on the chest wall. Basically the breast tissue consists of combination of fat and glandular tissue. The rest of the breast is made up of vascular tissue, connective tissue and nerves. Adipose (fat) tissue exists beneath the skin, back of the breast and between the glandular tissue. Glandular tissue in breast consists of lobs and ducts. Mostly cancers expand in the region of glandular tissue. The skin thickness varies between 0.8mm and 3mm in breast amd nipple is considered part of the skin which is surrounded by areola. Vascular and nerve tissue are effective for blood circulation.

3.2 Biology of tumor growth

The first step for detecting a breast cancer is to discover the tumor. Hence, it is essential to learn about tumor biology. In this section the biological basis of tumor growth is investigated. The growth of tumor, normally begins with a production of an abnormal cell in the process of cell division. The produced cell has the ability to reproduce itself rapidly. It will be raised

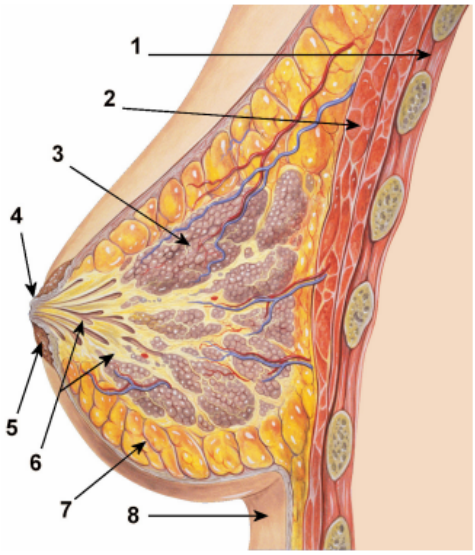

Figure 3.1. Breast Anatomy: 1. Chest wall 2. Pectoralis muscles 3. Lobules 4. Nipple 5. Areola 6. Ducts 7. Fatty tissue 8. Skin [1]

in form of in-situ lump which is characteristic of early stage tumors [16]. Breast tissue is a suitable place for cancer cells to develop rapidly. This is due to fact of female hormone estrogen. Estrogen provides an environment which advances rapid cell devision and increases the risk of cancer.

During stages of tumor development, it looks like a compressed sphere shape . In the early stages, tumor needs oxygen, amino acid and glucose for expanding. Mentioned nutrients are supplied by diffusion from healthy tissue and tumor. Depending on body situation, diffusion process may only secure the outer space of tumor cells or it may infuse to the center of the cells. In case of outer space of tumor cells, tumors can stay inactive in body for many years. Statistics show that tumors tend to grow more like a sphere. Therefor, in next section tumors are simulated in sphere form.

3.3 Modeling of Breast Tissue

Finite element analysis is a computational method. In this method, reaction of the model to real forces and fields is predicted. It is capable of accurate modeling and solving non-linear problems. In general, FE method(FEM) divides the full problem into smaller divisions and show the field in each sub-region. In this research, FEM solves the maxwell's equation particularly. Due to the multilayer structure of the breast model, it is difficult to calculate fields and energy through analytical approach. Therefor, FEA method is applied in this section to model and analyze the electromagnetic behavior of breast tissue.

Breast Model

Figure 3.2 illustrates normal breast tissue developed using Ansys software. It consists of main layers of breast: skin, fat and gland. Each layer has their own dielectric properties which has been considered in modeling.

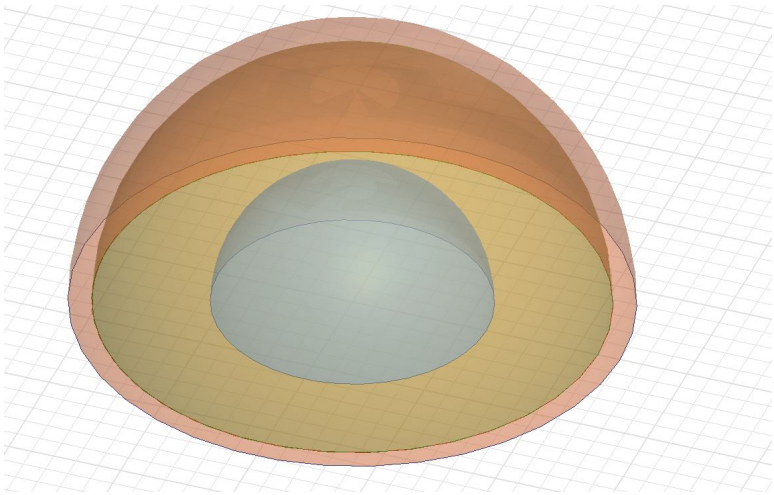

Figure 3.2. FEA breast model

Tissue materials in human body are frequency and temperature dependent. These dependencies are considered in defining material properties of the breast tissue. Several frequency-dependent material methods are provided through Ansys. In this research, one of the Ansys

methods is used which is called: "enter frequency dependent data points" method and it is an arbitrary piecewise linear model. This method consists of three main segments: flat, linear and flat. In other words, dielectric properties values are specified at an upper and lower corner frequency. Needed data points are imported from excel file to Ansys. Figure 3.3 and 3.4 show graphs of imported conductivity and permitiivity of skin and breast's fat. Both conductivity and relative permittivity are assigned to skin, fat and gland by using the mentioned method.

For thermal dependency, dielectric loss tangent is added to materials. Dielectric loss tangent represents how much power is dissipated in high-frequency electric field. It varies with frequency. To simulate the variances, a function for dielectric loss tangent is defined and imported to the material properties. Equation (3.1) shows the function of dielectric loss tangent. It is the ratio of real and imaginary part of permittivity. The smaller loss tangent, the less lossy the material.

$$Loss\ tangent = \frac{\epsilon"}{\epsilon'} \tag{3.1}$$

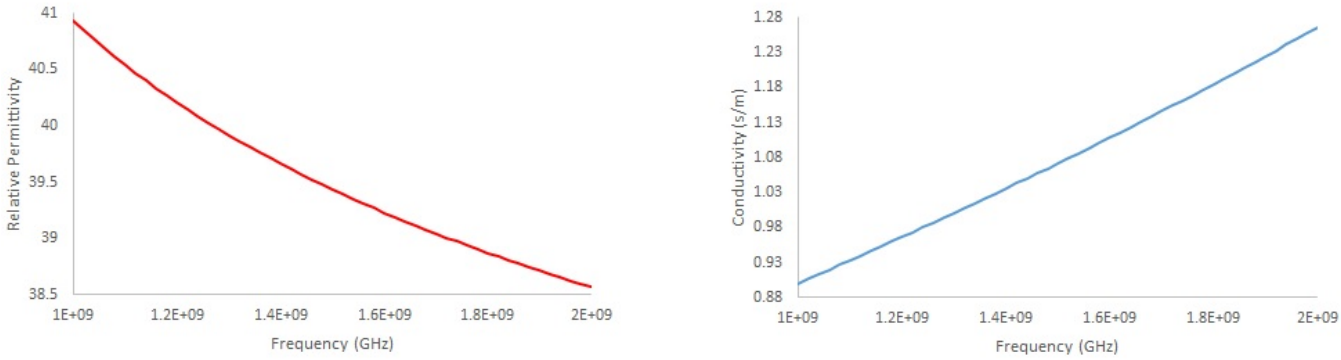

(a) (b)

Figure 3.3. Dielectric properties of skin vs frequency (a) Relative permittivity (b)Conductivity [2]

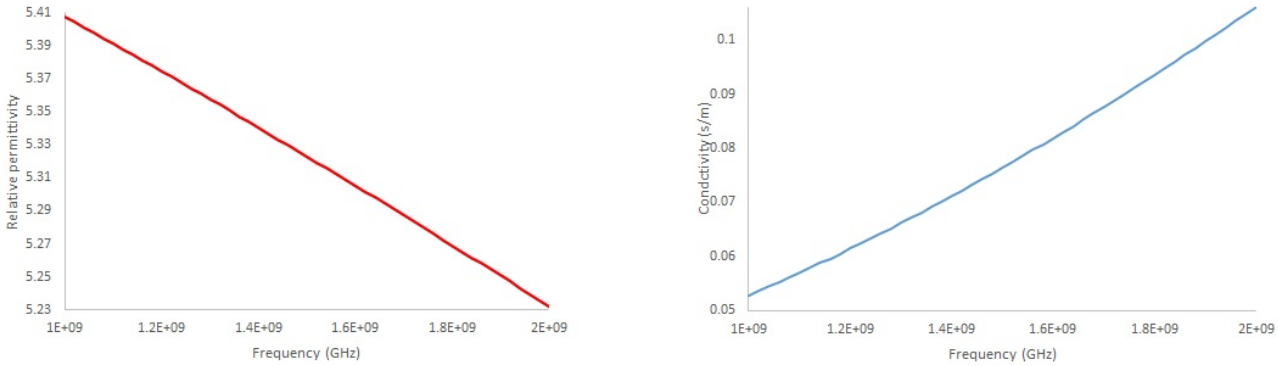

(a) (b)

Figure 3.4. Dielectric properties of breast's vs frequency (a) Relative permittivity (b)Conductivity [2]

As mentioned, the aim of research is to develop an innovative breast cancer detection method. Therefore a malignant breast tissue needs to be modeled to provide better comparison. Figure 3.5 illustrate a homogeneous and heterogeneous malignant breasts. Material properties of malignant breast is same as normal tissue, except for the tumor. Tumors dielectric properties are very similar to gland material which makes detection hard in some cases.

Tumor size and location are different for each patients and they change based on the cancer level. In order to have more realistic simulation, tumor size and positions will vary in each simulation. In next chapter, effects of tumor size and location on cancer is explained in more detailed.

The accuracy of simulation and model may depend on mesh size. In another word, solutions that use meshes with many small triangles and rectangles are more accurate than meshes with few elements. Figure 3.6 depicts the mesh of simulated breast model, the right side picture shows the surface mesh and the left one shows inside mesh of the model. Inside mesh plays an important rule in terms of transmission and reflection measurement. Provided

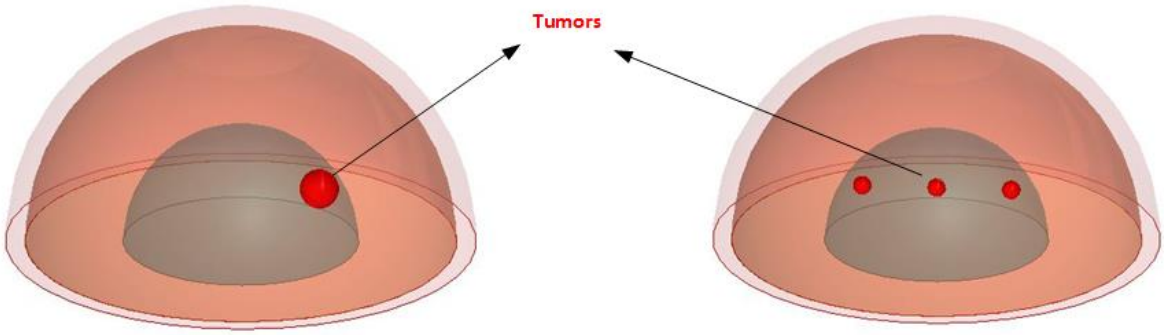

(a) (b)

Figure 3.5. Malignant breast tissue model (a) Homogeneous (b) Heterogeneous

results in next section, are based on skin depth-based mesh refinement. In skin depth-based mesh refinement , a layered mesh is assigned on the surface of mesh. The layers are arranged base on specific skin depth and number of the defined layers. In this simulation skin depth is equal to 4mm and number of layers element is 1000.

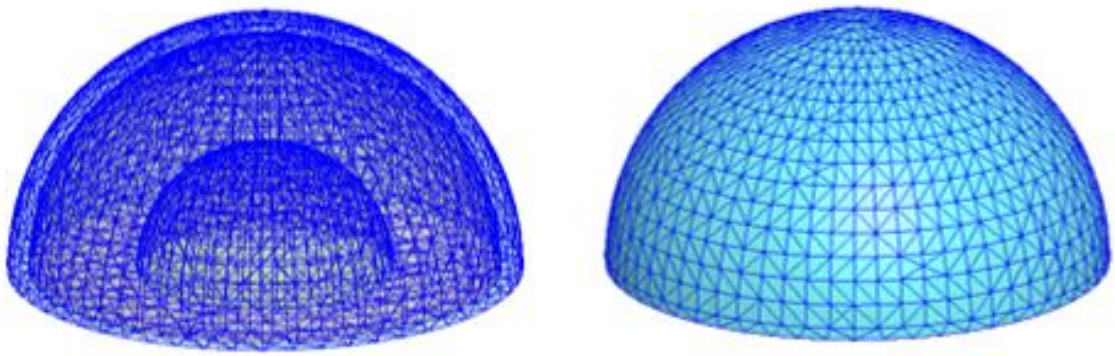

Figure 3.6. Mesh of simulated model

3.4 FEA of Breast Tissue

One of the key factors for breast cancer detection with RF filed interaction is comparison of dielectric properties in normal and malignant breast tissue. This comparison can be made by measuring SAR. SAR and absorbed power values determine the existence of tumor. In this section, EM analysis for normal and malignant breast is performed. Furthermore, their effects are studied.

The Ansys SAR measurement methods are explained below to have a better understanding of simulation results. It calculates SAR in two ways:

1. LocalSAR : It is calculated at each mesh points via the following Equation:

$$LocalSAR = \frac{\sigma(x,y,z)|E(x,y,z)|^2}{2\rho(x,y,z)} \tag{3.2}$$

   -where σ is the electrical conductivity of the dielectric material, E is the peak phasor electric field and ρ is the density of the dilectric material.

   Figure 3.7 depicts the localSAR calculation process. Ansys measures localSAR at each point on an overlay field and values between the mesh points are interpolated.

2. Average SAR: It measured average of SAR over a volume surrounding at a selected point. Averaging volume is specified by mass and material density of the tissue.

3. Certification SAR: After finding the maximum of localSAR on the surface of object, an averaged volume is produced around the maximum localSAR location. By having computed localSAR, Certification SAR is calculated inside the averaging volume.

Surface of cancerous breast tissue generates more heat compared to the healthy tissue. This is due to the fact that blood supply is increased. This temperature rise is reflected on the skin surface temperature and absorbed power. The generated heat also affectss SAR of the breast. Through the finite element simulation, it has been shown that the cancerous breast has a higher SAR than normal breast.

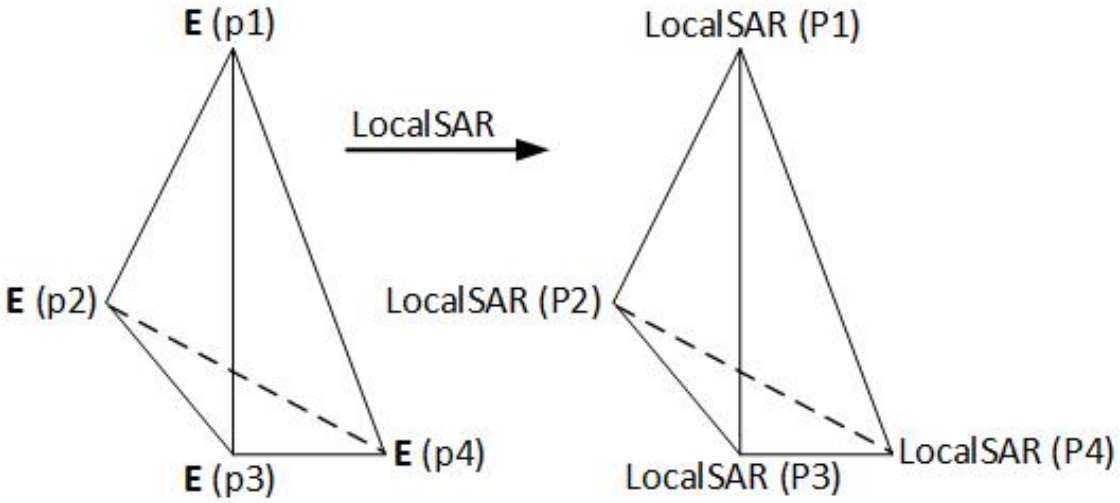

Figure 3.7. Demonstration of LocalSAR computation

Figure 3.8 shows local and average SAR of normal breast tissue. These fields are plotted on surface of skin. Both breast models have been excited with the same antenna and frequency. Size of skin, fat and gland tissue in them as shown in table 3.1. The only difference is the existence of a 10mm (radius) tumor in the cancerous tissue. This tumor caused the localSAR to be 43.14 % higher in cancerous breast tissue. Furthermore SAR value has not exceeded the standard limits.

From this figure, one of the elements for breast cancer detection is distinguished. In the next chapter, the effect of tumors location and size on SAR is discussed in more details and based on this we can say either a breast tissue is cancerous or not.

Table 3.1. Breast tissue dimension

Tissue type	Skin	Fat	Gland
Tissue thickness (mm)	5mm	25	30

Another important elements that would change when a tissue becomes cancerous is volume loss density. It can be calculated from Equation (3.3). It measures dielectric losses at high frequency and estimates how much power is lost in some volume of our model due to antenna

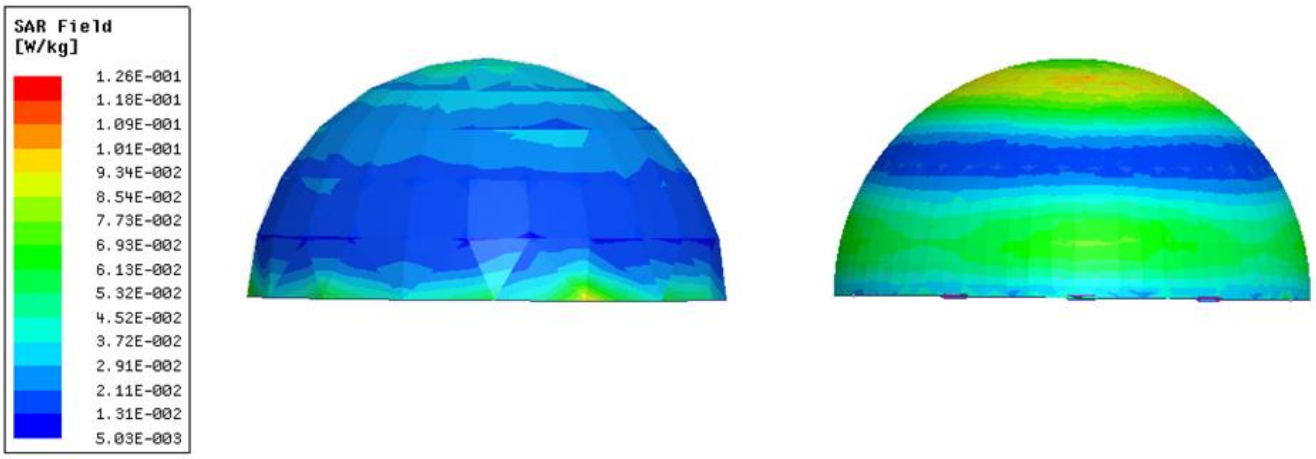

(a) (b)

Figure 3.8. LocalSAR on skin surface of (a) Normal breast (b) Cancerous Breast

radiation. In Figure 3.9 volume loss density of cancerous and normal breast is depicted. An arc is drawn on the edge of skin which shows that breast with tumor looses more power than normal one. Higher volume loss density appears on a breast with tumor because tumor tissues has higher energy compare to other type.

$$p_v = \frac{1}{2} Re(E.\widetilde{J} + jwB.\widetilde{H}) \tag{3.3}$$

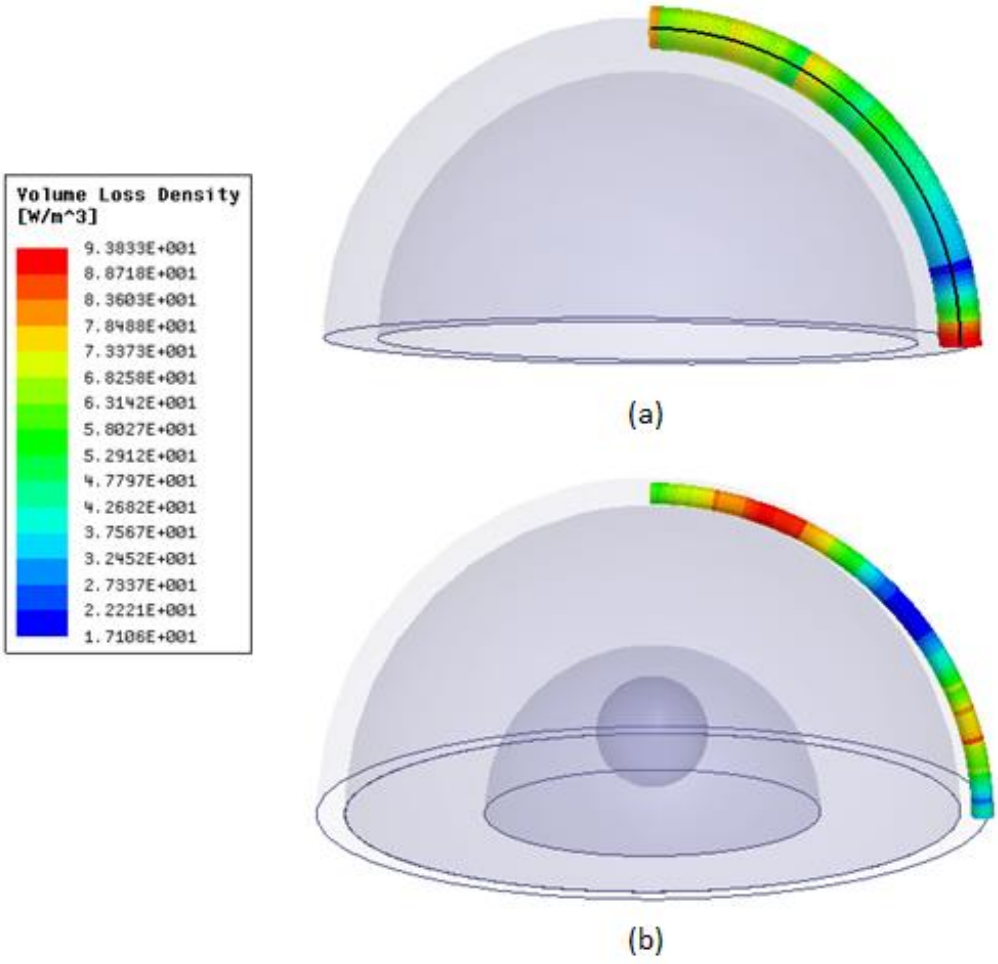

Figure 3.9. Volume loss density on (a) normal and (b) cancerous breast tissue

3.5 Summery

In this chapter a three-dimensional model of breast was introduced and solved for electromagnetic analysis under various condition using Ansys. The SAR for normal and cancerous breast tissue was analyzed. The behavior of malignant breast tissue was analyzed next, and it was distinguished that the tumor existence can be predicted by SAR value.

CHAPTER 4

DESIGN METHODOLOGY

4.1 Introduction

Effective breast cancer detection is part of the daily struggle in oncology field. Every woman needs to do breast examination several times in a year. As the technology advances, many detection methods have been invented and used. Most of the existing methods are not affordable and lack some features such as patient safety and precision. Furthermore, women can not self examine at home with available devices in market. Hence a cost effective and precise method with accurate design is needed in the women society to satisfy their needs and prevent the breast cancer by early detection. The aim of this chapter is to provide a method which can be applied as a wearable device for breast cancer detection.
In this chapter the design process and detection method are explained in terms of simulation and experimental results.

4.2 Methodology

Az mentioned in introduction chapter, there are two main types for breast cancer detection:

- Electromagnetic technique
- Thermal technique

Both of the above techniques have their own benefits and drawbacks which has been discussed in the first chapter.
Early breast cancer detection, is one the biggest concern in today's world. Hence, in this

chapter, an accurate and applicable method has been determined which combined both main techniques. The benefits of this combination is to achieve less health risk for patients while obtaining accurate results. In the next section, details of proposed method has been explained. [16]

4.2.1 Methodology process

In Figure 4.1 a flowchart of the whole analysis and methodology is shown. In order to observe malignant breast tissue two analysis has been applied.

- EM analysis:

  In this part the breast tissue has been modeled with perfect meshing. Moreover dielectric properties of tissue is considered. The details of model, meshing and material properties is described in chapter 3. As shown in Figure 4.1 after designing the model, setting material properties and assigning mesh, a RF source is needed to excite the tissue. RF antennas are determined as RF source excitation in this research. Below are the list of designed RF antenna that are used, details of their design and characteristic will be discussed in next section.

  - Monopole antenna
  - Dipole array antenna
  - Patch antenna

  Breast tissue is impacted by RF antenna which cause an excitation in different layers of it. Different layers in breast has different response to the RF excitation. By comprising their responses, signs of tumor existence are identified. The RF excitation is transformed to the power (Loss volume density) and transfered for thermal analysis.

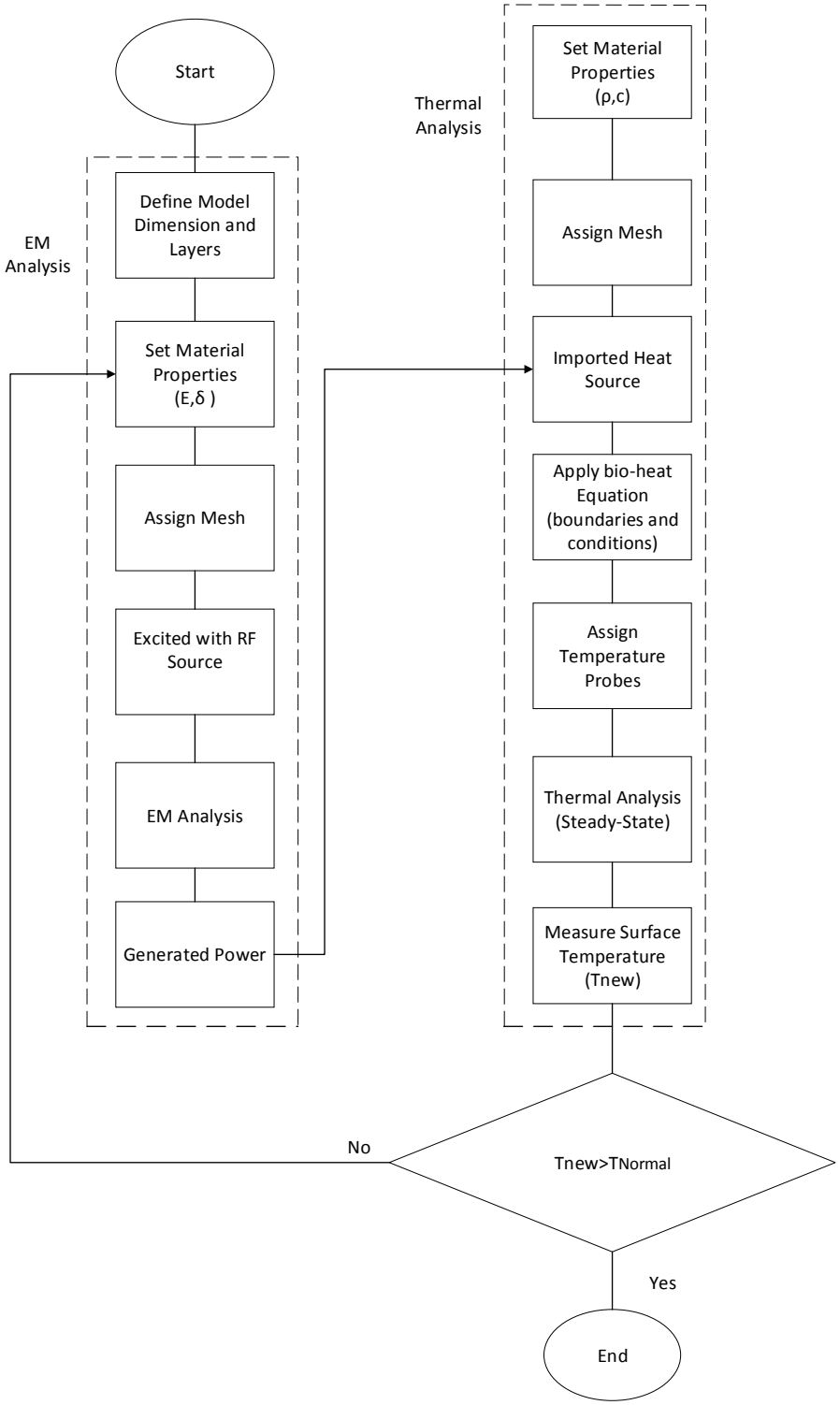

Figure 4.1. Flowchart of simulated model

- Thermal Analysis:

  Studies show that temperature variation in breast tissue can lead to the breast cancer detection. In 1963, scientists discover there is relationship between degree of malignancy of a tumor and temperature rise. This fact discovered during mastectomy operation by using the direct thermistor thermometery technique [16]. Furthermore, in [20] surface temperature distribution in breast cancer has been studied both theoretical and experimentally. In this study an artificial heat source implanted in human body and distinguished the skin temperature is related to the depth and power of the heat source. Base on the existing studies, it is obvious that surface temperature of breast is influenced by the tumor. In this section a thermal analysis is being performed and determined temperature and tumor relation.

  As shown in Figure4.1, first material properties such as density, isotropic thermal conductivity and specific heat has been set for thermal analysis. Table 4.1 shows the value of these properties. Next step is mesh assignment.

Table 4.1. Thermal properties of breast tissue

Tissue	Density ($\frac{kg}{m^{-3}}$)	Isotropic Thermal Conductivity ($\frac{W}{mC}$)	Specific Heat ($\frac{J}{KgC}$)
Skin	1109	0.37	3391
Fat	911	0.21	2348
Gland	1058	0.33	2960
Tumor	1050	0.33	3000

Every accurate analysis must have an appropriate mesh assignment. EM results can not be imported to thermal analysis if the meshing is inaccurate. Therefor different types of mesh is applied in this simulation. Below is the list of applied mesh.

- Mesh refinement: It is a mesh generation process in which elements are divided on the surface of each layer. This is an effective method for controlling mesh of edges and faces.

- Face sizing : This methods controls the mesh size distribution. The angel between mesh elements is set. Furthermore number of applied mesh elements in the gaps between two geometric section is determined,
- Patch control: It uses an algorithm which refines the mesh elements and avoids unnecessary meshing. Patch mesh makes the computation faster. Figure 4.2 shows all the assigned mesh in the simulation.

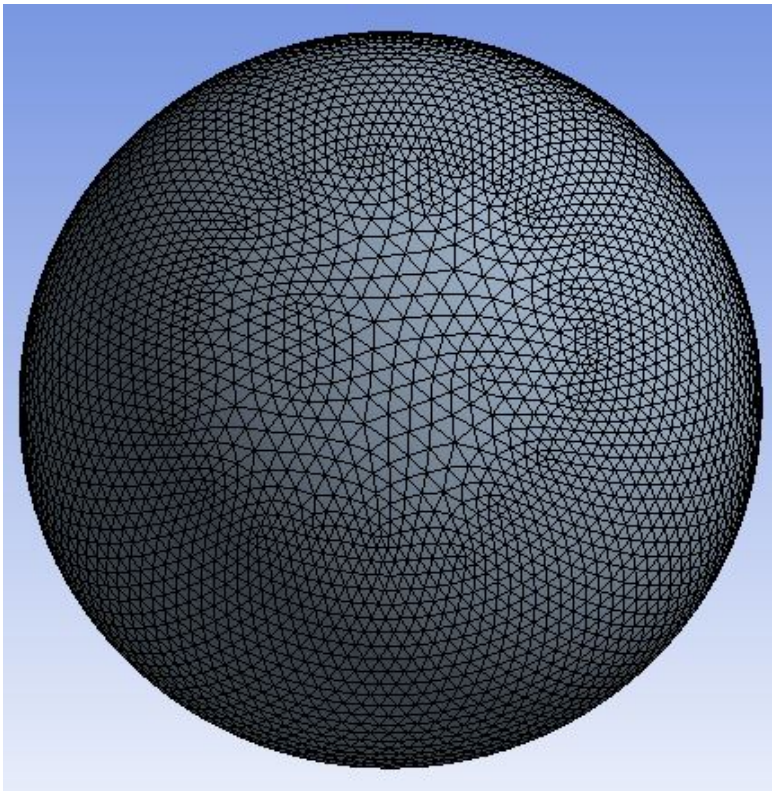

Figure 4.2. Mesh of simulated model

After assigning mesh, generated power imported completely from EM analysis and bio-heat equation is applied. In section of sensitivity analysis of thermal analysis results will be shown.

4.2.2 RF Sources

Three types of RF antennas are designed and simulated. All of them are placed on top of the breast tissue. In below a brief description of their design and simulation results are explained.

Monopole Antenna

Monopole antenna is one of the basic and useful antenna in RF industry. It is half of a dipole antenna and most of the time is is mounted perpendicular to some sort of conductive plane (ground plane). Since it is a resonant antenna the length of the antenna is defined by wavelength of the used radio waves. The transmitting or receiving signal is applied through the lower end of the monopole and conductive plane. As shown in Figure 4.3 one side of the antenna is connected to the end of monopole and the other side is connected to the ground plane. In this part a wire monopole is simulated as shown in Figure 4.3. The center frequency for this antenna is 2.4 GHz and its size specification is mentioned in table 4.2

Table 4.2. Monopole antenna dimension

Monopole Length (cm)	Monopole Radius (cm)	Feed Gap (cm)
3.26	0.1	0.1

Dipole Antenna Array

It is one of simplest and convenient antenna in telecommunications and radio application. It is similar to monopole except that it consists of two conductive elements, also it is a resonant antenna and the length of it can be calculated by wavelength of the radio waves. The radiation pattern of a dipole is omnidirectional. In this research dipole antenna array

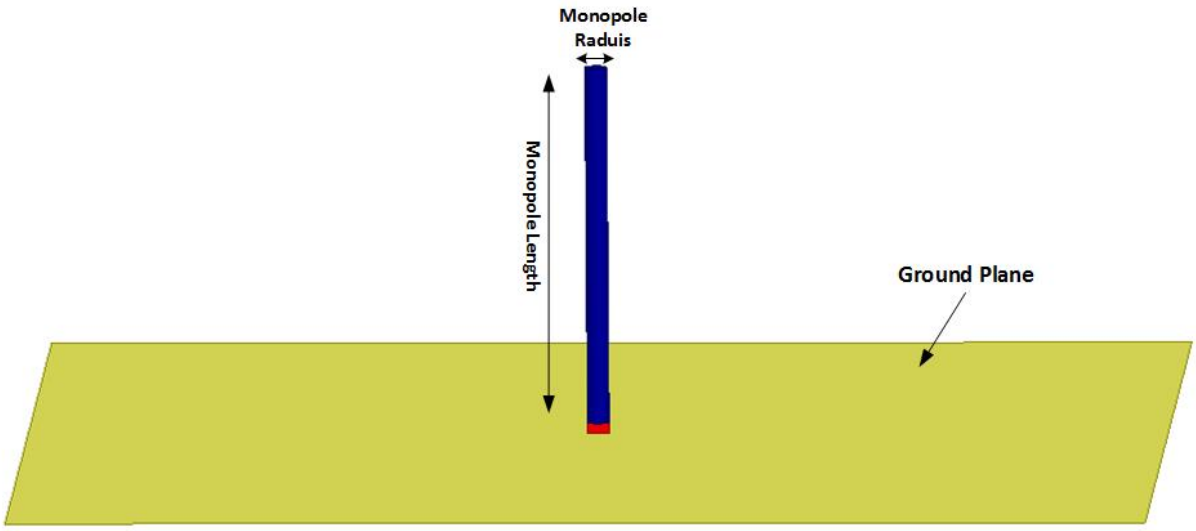

Figure 4.3. Monopole Antenna

is simulated and the dipole length of each antenna is approximately 0.25 of the wavelength. Array antenna has higher gain and is capable to radiate in specific direction more precisely. Figure4.4 depicts simulated antenna array. As shown it consists of four dipoles antenna, ground plane and an airbox. Airbox is assigned to determine radiation boundary condition. Figures 4.5 and 4.6 show that design has robustness and all of the antennas have approximately same return loss. A small shift in frequency can be seen from S11 to S33 and S22 to S44, which is negligible. This is due to the fact of radiation pattern in array and this fact can not cause a false in simulation results. All of the four dipole antennas are working delicately at their center frequency.

As mentioned, arrays are capable of producing higher gain. Figure 4.7 shows a gain comparison of simulated dipole antenna array and monopole antenna. Dipole array antenna has 72.308 % more gain than monopole antenna. Higher gain is useful for sensitivity analysis which can bring accurate results. Total antenna gain for is calculated over sweep of theta. In monopole antenna case theta is between -200 to 200 degree and for dipole array antenna is

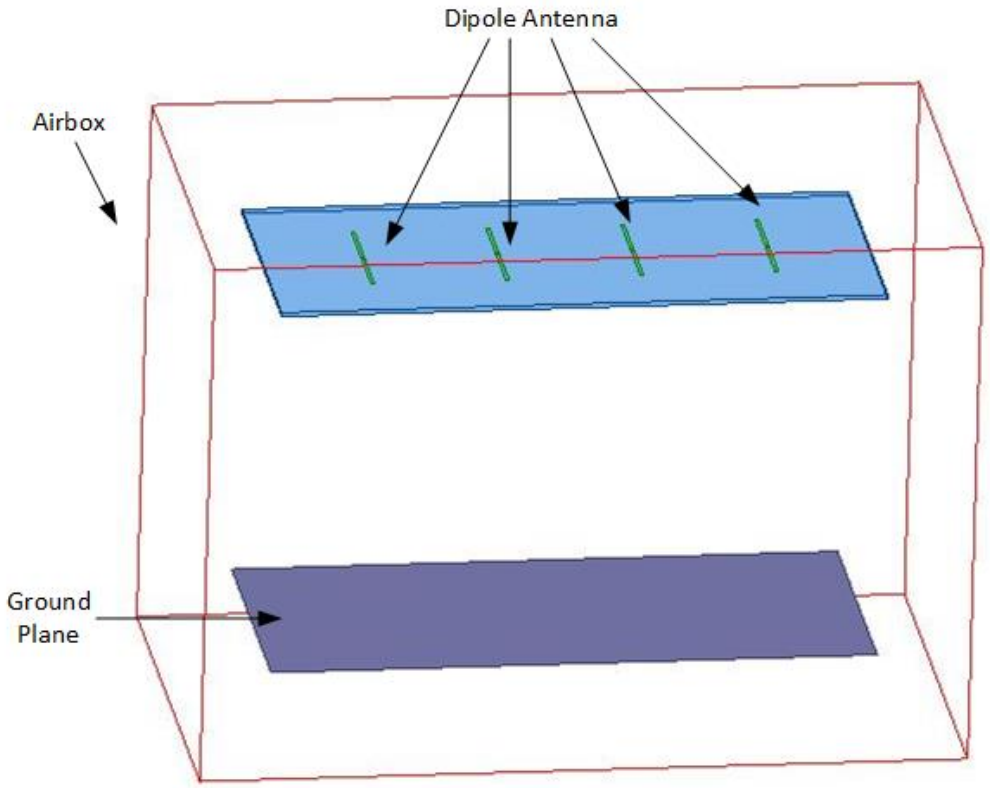

Figure 4.4. Simulated Dipole Antenna Array

between 0 to 180 degree. It is important for breast tissue to get the RF signal from specific radiation source. In this research, dipole antenna array plays as specific radiation source.

Patch antenna

An antenna that can be mounted on a flat surface is one of the needs in researches and industries. Patch antennas are becoming interesting to manufacturer because of their shape and ability to mount on a flat surface. They have been widely used in many applications such as mobile phone market because of their low cost, low profile and easy fabrication. Therefor it is effective to design and test a patch antenna for the proposed method.

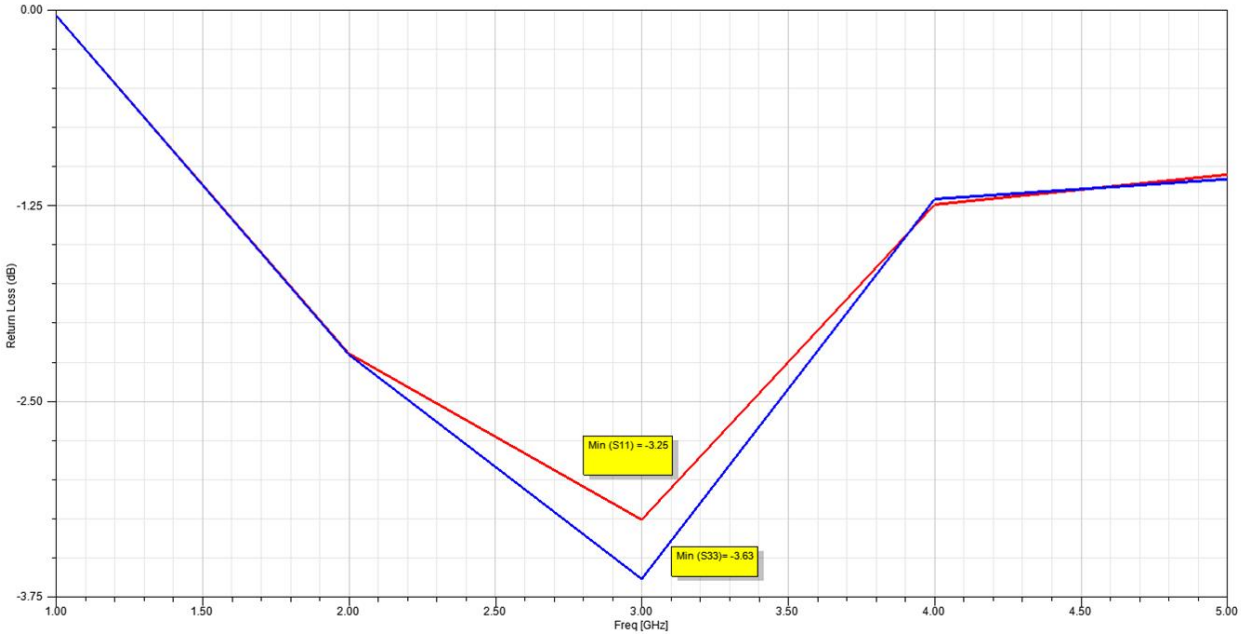

Figure 4.5. Return Loss of 1st and 3rd dipole antenna

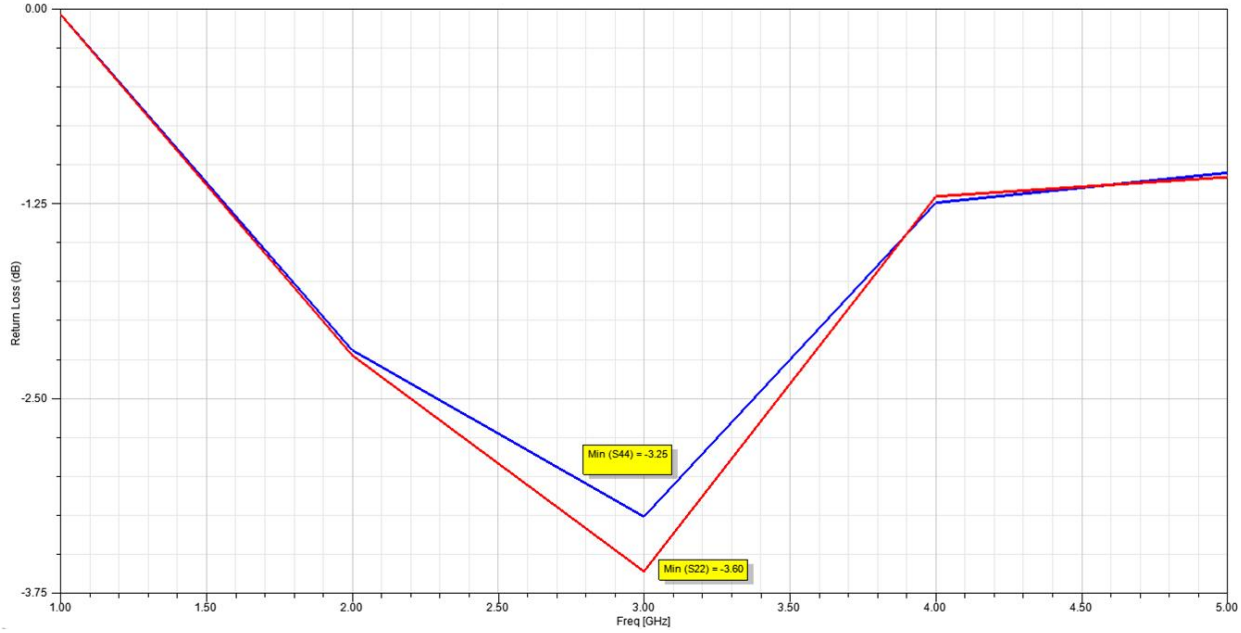

Figure 4.6. Return Loss of 2nd and 4th dipole antenna

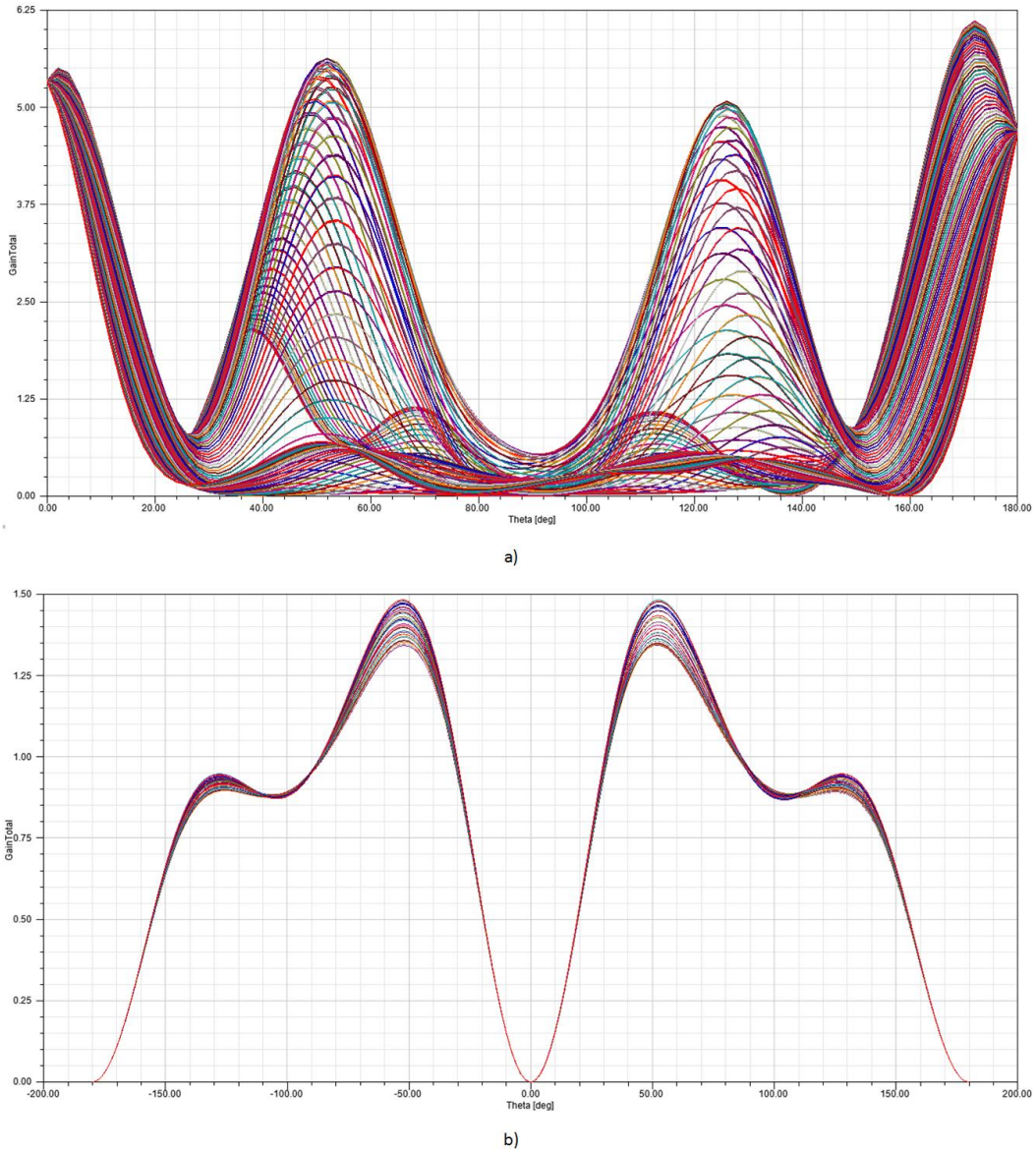

Figure 4.7. Total gain of a) dipole array antenna b) monopole antenna

As shown in Figure 4.8 patch antenna is fed by a microscopic transmission line. All

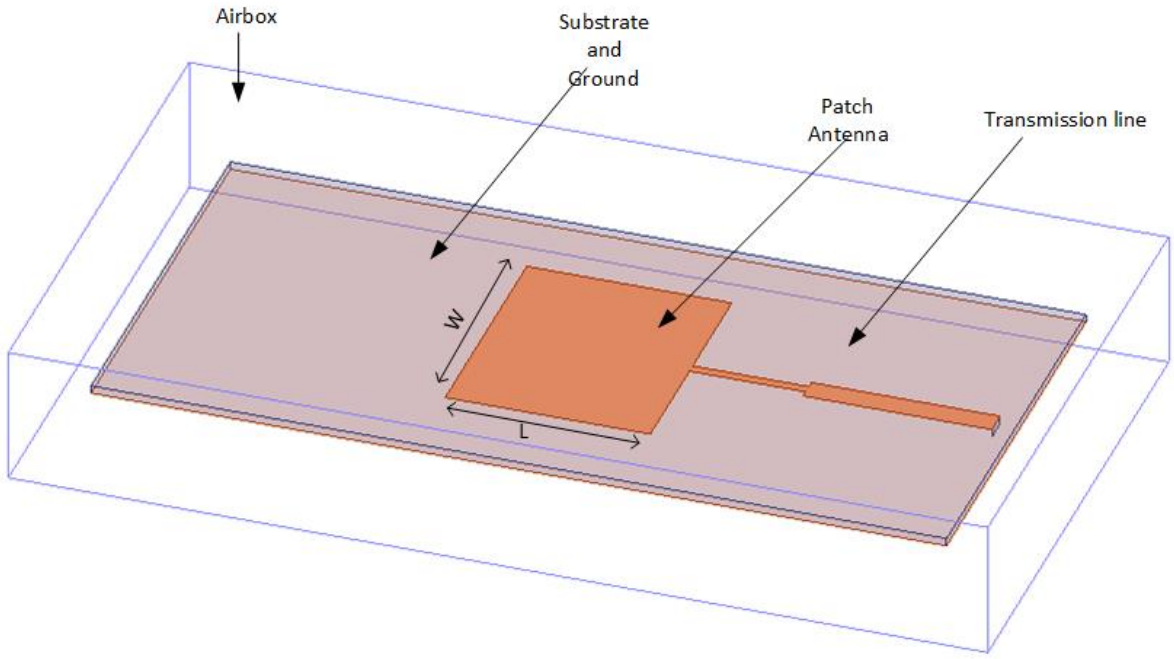

Figure 4.8. Simulated patch antenna

parts(Antenna, transmission line and ground plane) of patch antenna are made of high conductivity materials such as copper. In the simulated antenna, thickness of patch antenna is approximately equal to 0.013 of the wavelength which is a good design and will not effect the antenna efficiency. The length and width of the antenna are calculated by Equation (4.1) and (4.3), where c is speed of light,f_0 is the operation frequency and ϵ_r is dielectric constant which is equal to 2.2, h is the thickness of the antenna which is equal to 62 mil, W is the width of the antenna and ϵ_{eff} is calculated by Equation (4.2).By applying mentioned equation, width and length are respectively equal to 4.74 cm and 3.97 cm.

$$Width = \frac{c}{2f_0\sqrt{\frac{\epsilon_r+1}{2}}} \tag{4.1}$$

$$\epsilon_{eff} = \frac{\epsilon_r + 1}{2} + \frac{\epsilon_r - 1}{2}[\frac{1}{\sqrt{1 + 12(\frac{h}{W})}}] \tag{4.2}$$

$$Length = \frac{c}{2f_0\sqrt{\epsilon_{eff}}} - 0.824h(\frac{(\epsilon_{eff} + 0.3)(\frac{W}{h} + 0.246)}{(\epsilon_{eff} - 0.258)(\frac{W}{h} + 0.8)}) \tag{4.3}$$

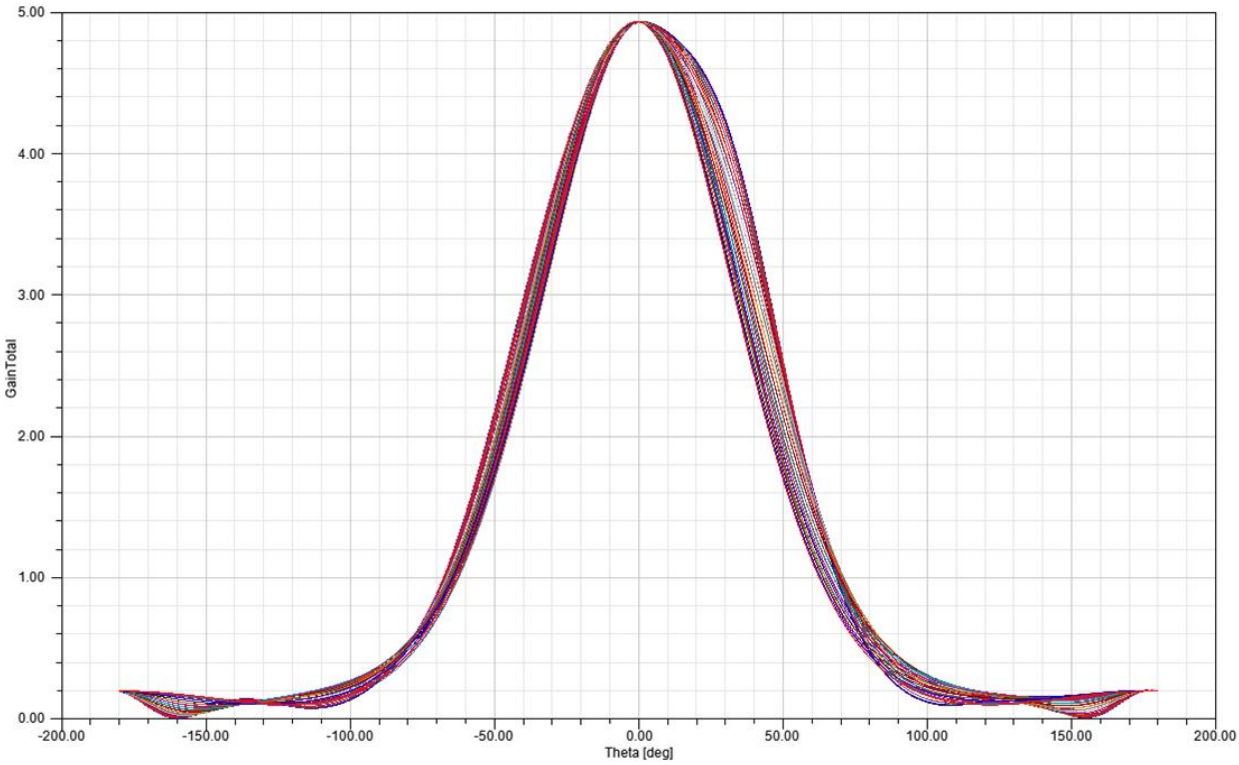

Figure 4.9. Total gain of patch antenna

The patch antenna has been selected for this research because of its shape and gain. Moreover different types of antenna needs to be tested for a sensitivity analysis. The gain of simulated patch antenna is near to the dipole array antenna with a lower center frequency. Figure 4.9 shows a plot of total gain over theta sweep. Theta is between -180 to 180. Furthermore patch antenna return loss(S11) is higher than dipole array antenna which means it can radiates more. Resonant frequency(f_c) is equal to 2.43 GHz base on Figure4.10 and below Equation

proves that simulated patch antenna worked properly around its desired resonant frequency (f_c).

$$f_c \approx \frac{c}{2L\sqrt{\epsilon_r}} = 2.5GHz \tag{4.4}$$

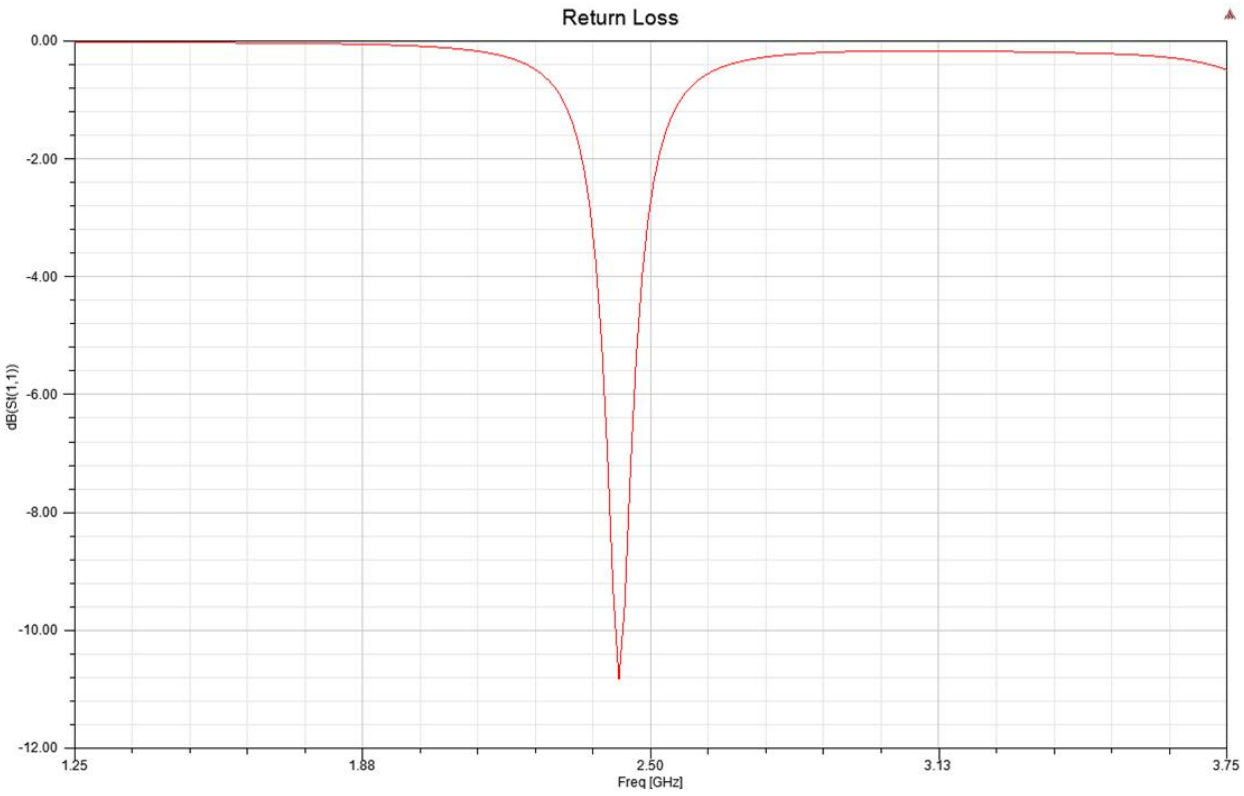

Figure 4.10. Return Loss of patch antenna

4.2.3 Thermal sensor pattern

As mentioned the proposed method is based EM and thermal analysis. In this section the temperature sensor pattern is explained and depicted. Eighteen temperature sensors are assigned on the surface of the breast skin to analyze the temperature variation due to size, number and location of the tumor.

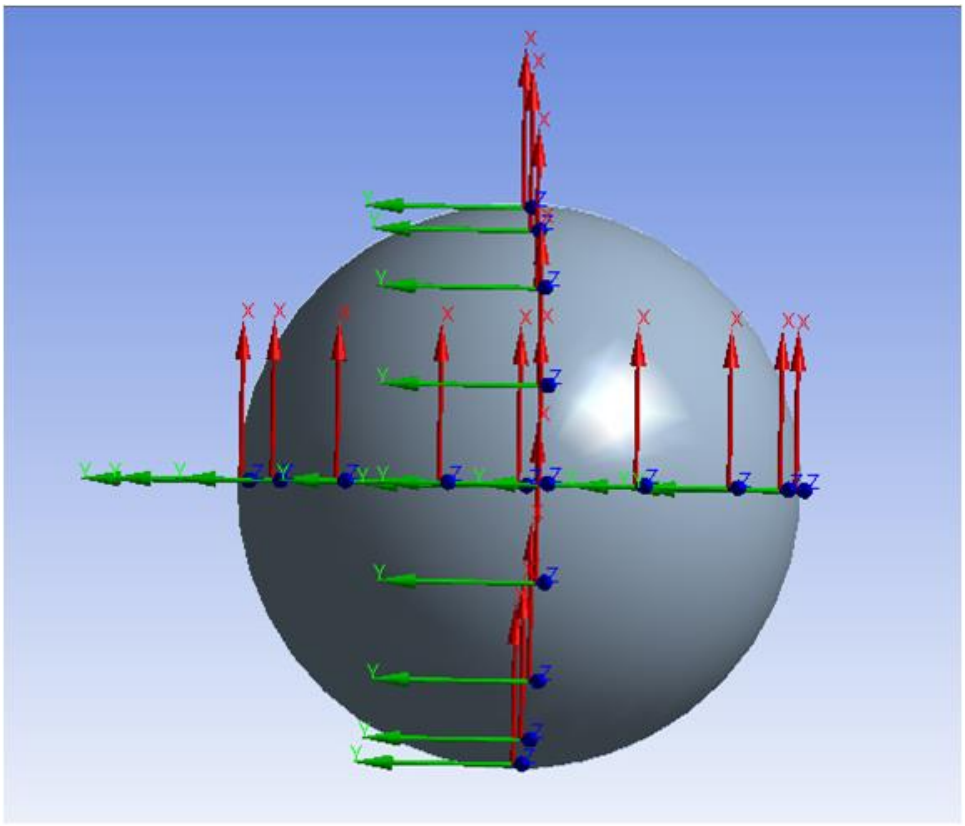

Figure 4.11. Temperature Sensors Placement

Sensors are attached on ±YZ and ±XZ planes as shown in Figure4.11. The distance between sensor temperature and bottom of the breast is measured by Equation(4.5), where P refers to an arc from bottom to desired point and θ is the angel between bottom and desired point and θ unit is radian.

$$P = Raduis * \theta \tag{4.5}$$

Table 4.3 shows the exact position of temperature sensors in ±YZ and ±XZ planes. All of the values are measured in meter(m).

Table 4.3. Position of temperature sensors

Temperature Sensors	X	Y	Z
T_1	0	0.0600	0
T_2	0	0.0554	0.0229
T_3	0	0.04242	0.0424
T_4	0	0.0229	0.0554
T_5	0	0	0.0600
T_6	0	-0.0600	0
T_7	0	-0.5543	0.0229
T_8	0	-0.04242	0.0424
T_9	0	-0.0229	0.0554
T_{10}	0.0600	0	0
T_{11}	0.0554	0	0.0229
T_{12}	0.04242	0	0.04242
T_{13}	0.0229	0	0.0554
T_{14}	-0.0600	0	0
T_{15}	-0.05543	0	0.0229
T_{16}	-0.04242	0	0.0424
T_{17}	-0.0229	0	0.0554

4.3 Sensitivity analysis

A sensitivity analysis is a technique used to determine how different values of an independent variable impact a particular dependent variable under a given set of assumptions. This technique is used within specific boundaries that depend on one or more input variables. In this research a sensitivity analysis is done to determine impact of tumors location, size and numbers on a breast tissue.

4.3.1 Effect of Tumor Size

Tumor size is an important factor for determining the stage of the breast cancer. As the size of a tumor extends the level of malignancy in breast tissue becomes worst. Therefor, a sensitivity analysis is performed to investigate the relationship of the surface temperature and tumor size.

Three different size of tumors with radius of 2.5, 7 and 10 mm is defined inside of the breast model. In order to simplify the sensitivity analysis, all of the tumors have the same center position. Figure4.12 shows tumors with different sizes and located 15 mm away from origin at point (0, 0, 15) mm.

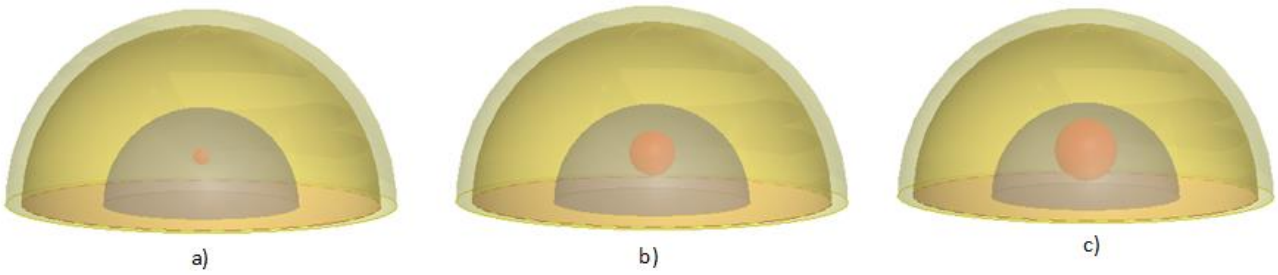

Figure 4.12. Tumors Inside Breast Model with radius of a)2.5 mm b)7 mm c)10 mm

Simulation results show that as the tumor size increases, surface temperature increases.This is due to the fact that temperature depends in metabolic heat activity and vascular circulation of tumors. Cancerous breast tissues metabolic heat generation rate are different from normal breast tissues. Therefor, they cause a higher temperature on surface of breast skin compare to a normal tissue. Table 4.4 [24] depicts temperature at the surface of breast tissue with respect to tumor size. These results clearly show that temperature increases with tumor size. Although it is hard to detect a tumor with radius of 2.5 mm in a breast with radius of 60mm. In this types of situation, other factors are needed for detection. SAR is one of the factors which could be effective and useful.

In the table4.4 all of the temperature are measured with two specific temperature sensors, T_2 and T_3 from Tabel4.3.

Table 4.4. Surface temperature versus tumors size

	Normal	2.5 mm tumor	7 mm tumor	10 mm tumor
T_2 $[°C]$	23.237	23.237	24.225	24.228
T_3 $[°C]$	23.047	23.047	23.857	23.861

4.3.2 Effect of Tumor Location

In this section, effects of tumor location on surface temperature is investigated. As shown in Figure 4.13 tumors with different sizes are moved from P_1 to P_2.

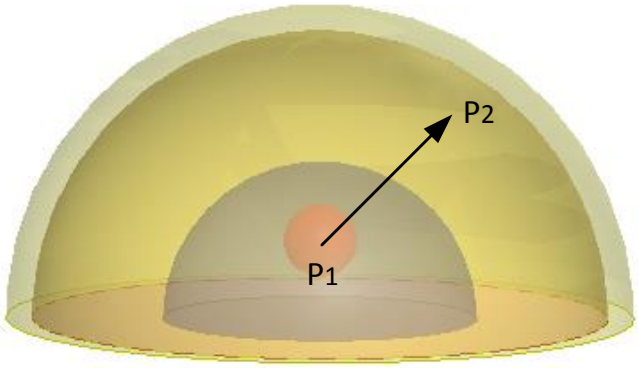

Figure 4.13. Tumor movement path

The surface temperature of breast model along with the distances from bottom is depicted in Figure4.14 [24]. In this figure, the surface temperature of different sizes (r, tumor radius) and locations(d, distance from origin) are shown . The results show that surface temperature varies as the tumor gets closer to the surface. In Figure4.14, ΔT refers to the difference between cancerous and normal breast tissue and P is measured by Equation 4.5.

4.3.3 Effect of SAR

The homogeneous breast is excited with dipole antenna array. Dipole antenna has better precision in measurement than other types RF source. This is due the fact of its gain and directivity. The average value of SAR is calculated for normal and cancerous tissue. A tumor

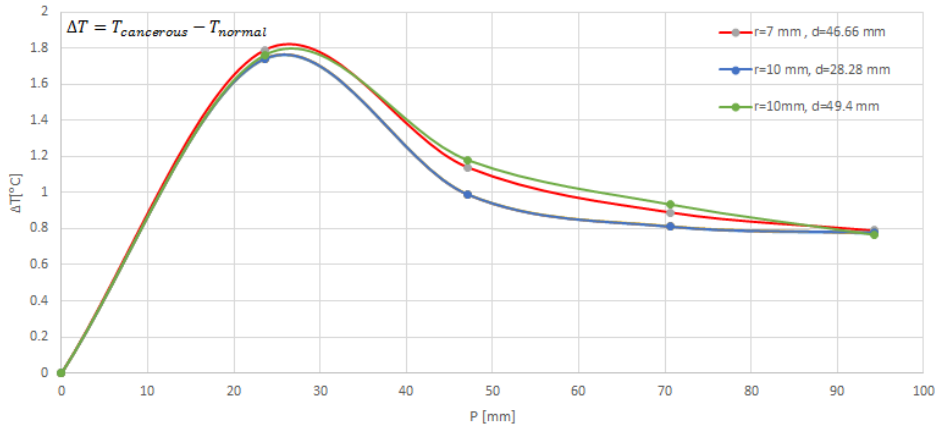

Figure 4.14. Surface temperature increase for tumors location

Table 4.5. Averag SAR in normal and cancerous breast tissue

Frequency (GHz)	**Normal Tissue (W/kg)**	**Cancerous Tissue (W/kg)**
1	0.2053	0.1431
1.2	0.2019	0.2551
1.4	0.1089	0.3892
1.6	0.0470	0.4486
1.8	0.0451	0.7539
2	0.0573	0.7127

with radius of 7mm is located 15 mm far away from the origin. Table4.5 summarizes average values of SAR for normal and cancerous breast tissue. It is observed average SAR values is higher in the cancerous breast compared to normal breast for frequencies above 1 GHz.

The same is done for higher frequencies in terms of maximum values. Table4.6 [24] depicts the value of maximum SAR in a normal and cancerous breast. It is observed that maximum SAR value is higher in abnormal breast tissue compared to normal breast tissue. The maximum SAR values have the same behavior as average SAR values. As a result, values of SAR at frequencies higher than 1 GHz can navigate to tumor location and determine the existence of the tumor. This is due to the fact that EF distribution has higher value near tumor. As explained in chapter 2 and 3, SAR is depended on EF values and distribution. Therefor, SAR values are helpful in detection of early tumors.

Table 4.6. MAX SAR in normal and cancerous tissue

Frequency (GHz)	**Normal Tissue (W/kg)**	**Cancerous Tissue(W/kg)**
1	0.365	0.354
2	5.459	6.102
3	6.880	10.500
4	9.408	9.814
5	8.870	9.016

4.3.4 Effect of Multiple Tumors

A heterogeneous breast with skin, gland, fat and multiple tumors is modeled. The size of 2.5 mm and 7mm are assumed for the tumors radius. In order to simulate the realistic scenario of cancerous breast tissue, locations of tumors have various locations and sizes.

Table 4.7. Scenarios of multiple tumors placement

Number of tumors	**Scenario 1**	**Scenario 2**	**Scenario 3**
2.5 mm	3	5	2
7 mm	0	0	1

To determine whether size and locations of tumors had any significant effects on surface temperature, several sensitivity analysis are performed. To prove the robustness of the simulation mesh, eighteen temperature sensors are applied for surface temperature measurement.All the shown temperature measurements are in Celsius[$^{\circ}C$]. In this section, three main scenarios has been defined. In Table4.7 number and size of tumors in each scenario is mentioned. Moreover, Figure4.15 depicts the formation of tumors. The locations and sizes are assigned randomly. In all of the scenarios, all of the properties of breast model except tumors remained the same.

In the 1st scenario, three tumors with radius of 2.5 mm are located at (0, 0,15) and (0,$\pm$10,15). As shown in Table4.8 temperatures are higher than normal breast tissue and cancerous tissue with one tumor breast. The maximum temperature difference increased 0.002 $^{\circ}C$ as the number of tumors increased from 1 to 3.

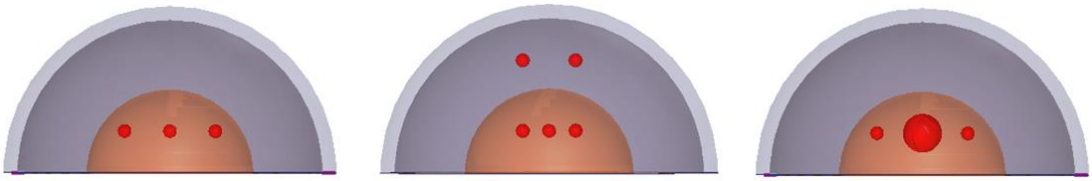

(a) (b) (c)

Figure 4.15. Tumor placement a) Scenario I b) Scenario II c) Scenario III

Table 4.8. Measured temperature in scenario I

Coordinate Plane	T1	T2	T3	T4	T5
YZ	37	24.639	23.236	23.052	22.996
-YZ	37	24.640	23.233	23.053	22.996
XZ	37	24.651	23.244	23.060	22.996
-XZ	37	24.638	23.232	23.050	22.996

In the second scenario, two more tumors are added to the first scenario which are located at (0,±10, 40). The results show that the presence of more tumors is always associate with an increase in surface temperature. Average temperature in scenario II is 0.003 $^{\circ}C$ higher than scenario I. Moreover, it is obvious that surface temperature of malignant breast tissue with five tumors is higher than normal breast tissue.

Table 4.9. Measured temperature in scenario II

Coordinate Plane	T1	T2	T3	T4	T5
YZ	37	24.644	23.241	23.060	23
-YZ	37	24.642	23.238	23.056	23
XZ	37	24.655	23.248	23.064	23
-XZ	37	24.644	23.236	23.055	23

In the third scenario, radius of the center tumor is increased from 2.5 mm to 7 mm. Table4.10 shows the measured surface temperature. Surface temperature of the same location in scenario III in higher than scenario I. It can be concluded that size of the tumor has more impact on surface temperature compare to the number of tumor.

Table 4.10. Measured temperature in scenario III

Coordinate Plane	T1	T2	T3	T4	T5
YZ	37	24.841	23.355	23.147	23.086
-YZ	37	24.833	23.351	23.147	23.086
XZ	37	24.837	23.353	23.141	23.086
-XZ	37	24.843	23.356	23.147	23.086

4.4 Experimental Results

The concept of "breast cancer detection with magneto-thermal modeling" was introduced previously. Moreover, the stability of this method is proven by simulation results. However, in terms of RF sources, simulation results can not guarantee that an antenna can work properly in desired frequency. Therefor, a patch antenna has been designed and implemented.

4.4.1 Patch antenna

Developing a patch antenna is divided into the design of the layout and fabrication of it. Although these two parts are separate. The layout design has been done with AWR software and fabrication part is done with ProMat instrument. Both of these sections are explained in more details in below.

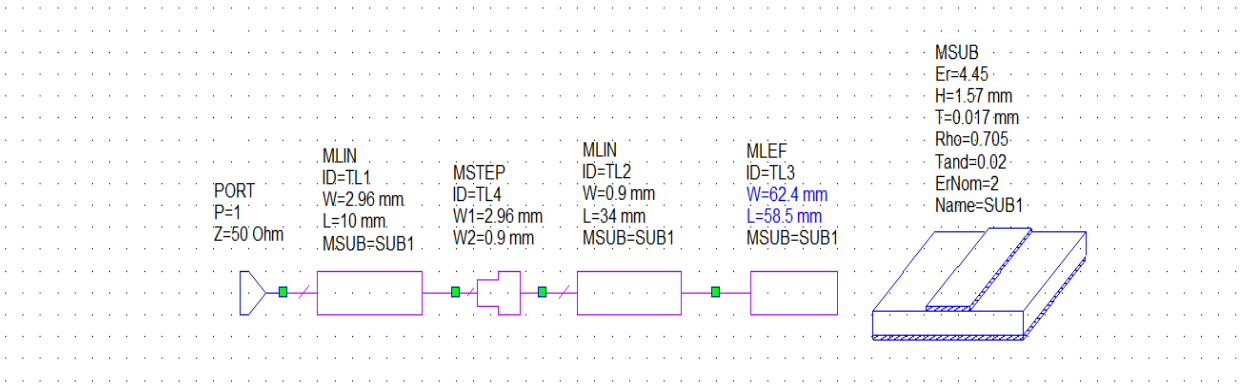

Figure 4.16. Layout blocks in AWR

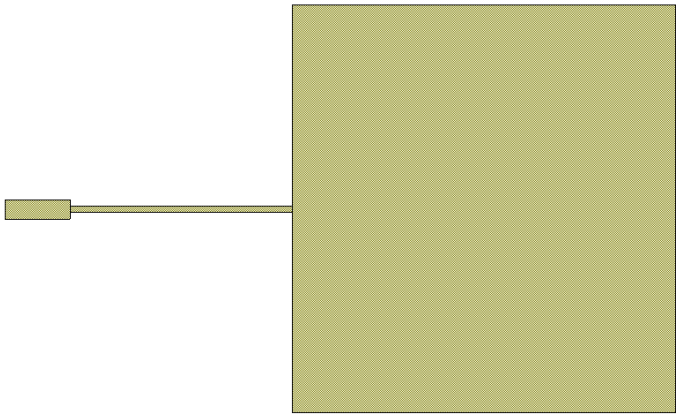

Figure 4.17. Layout of patch

The layout of the patch antenna is designed with AWR software. Different blocks for transmission line and patch area is used. Figure4.16 illustrates block diagram of designed layout and properties and dimensions of each block is shown as well. Finally, a two dimension view of layout is depicted in Figure 4.17.

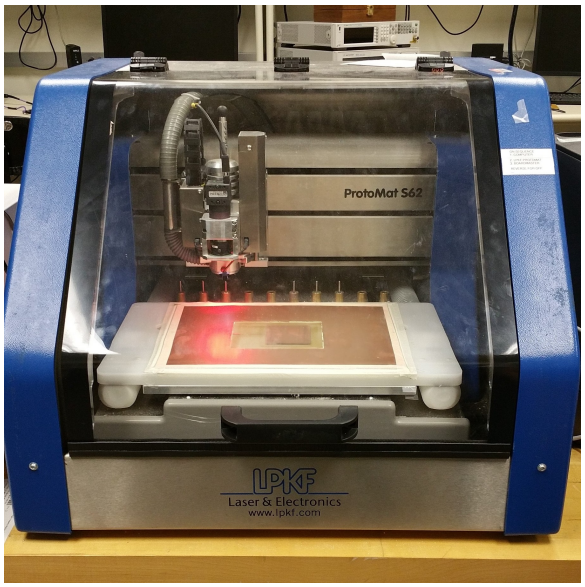

Figure 4.18. Patch fabrication with ProMat S62

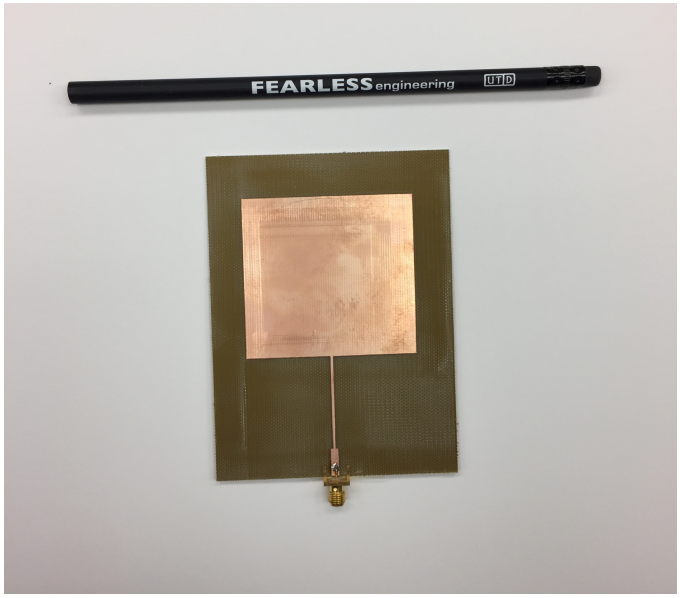

Figure 4.19. Fabricated patch antenna

As shown in Figure4.18, a prototype of patch antenna is fabricated with ProMat S62 (PCB Milling Machine) using high frequency laminate materials. The ProMAt S62 uses CAD data from BoardMaster software,convert layout data into actual printed circuit boards. This instrument has a recognition camera for alignment the sides of the patch antenna layout. Moreover, it has high accuracy tool changer for different parts of the board. Figure 4.19 shows the fabricated patch antenna. The dielectric substrata of patch antenna is made of FR4. FR4 is a composite material which is mainly uses for printed circuit boards.In order to test the antenna a vector network analyzer(VNA) is employed. Figure4.20 represents the measured S11 from VNA. It can be concluded and the antenna resonants at desired frequency and works properly.

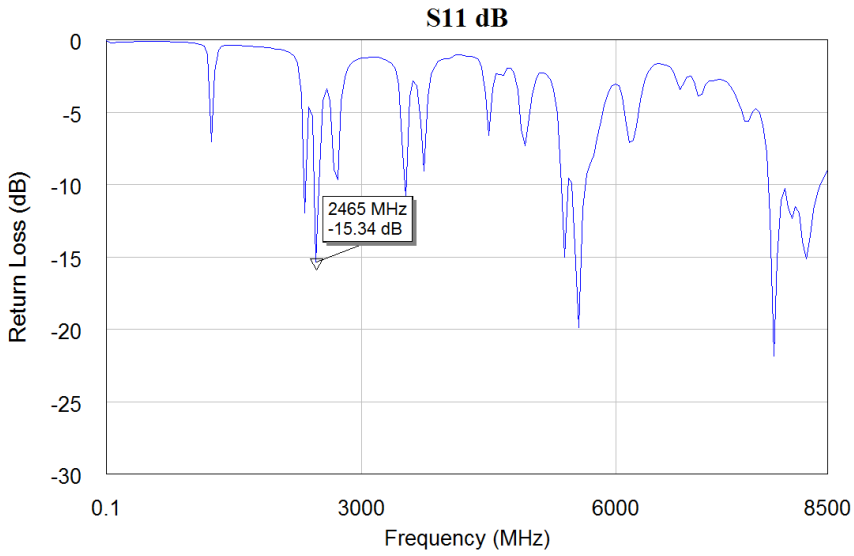

Figure 4.20. Return loss of patch antenna measured by VNA

4.5 Summary

In this chapter a new cancer detection method is introduced and investigated. Combining EM and thermal analysis is the key success factor of the proposed method. Detection strategy is base on significant dielectric and thermal contrast between normal and cancerous breast tissue. Details of proposed method is discussed and explained. Moreover, several sensitivity analysis are performed to prove the stability of it. Results show that SAR and surface temperature can navigate to tumor location size and area and temperature is a significant factor and can be correctly used for tumor detection.

CHAPTER 5

CONCLUSION

Breast cancer is a deadly disease that needs to be detected and controlled in the early stages. Unfortunately, many women suffer from consequences of this disease due to the financial factors and lack of comfort with existing detection procedures. An early stage detection of breast cancer can drastically increase the chance of a successful treatment of this disease. Investigation of the magneto-thermal behavior of biological tissues leads to a better understanding of breast cancer detection methods.

This research has been studied and proposes a novel method for breast that can overcome the shortcomings of current detection methods. By combining thermal and electromagnetic analysis, the proposed method can improve reliability and efficiency of breast cancer detection. A homogeneous and heterogeneous breasts tissues are modeled and excited with different types of radio frequency sources and thermal analysis is performed accurately by considering human metabolism. The simulation analysis demonstrates that the malignant tissue increases the surface temperature. Moreover, by using the distribution of temperature and specific absorption rate, it is possible to pinpoint the size and location of the cancerous tumors.

Proposed method can be utilized to design a wearable device that can be used anytime and anywhere to collect temperature and signals of breast tissue and analyse the data to estimate the chance of breast cancer . It enables women to perform a self examination test at home using this wearable device. Additionally, this device is designed to be convenient and easy to use. Th device is composed on the series of patch antennas and thermometers, which can excite the tissue, collect the reflective electromagnetic signal and measure the temperature on the surface.

Future studies can elaborate on characterizing the different types of errors which might arise in the analysis. Different factors such as patient's age, weight, air flow around breast and position can also have potential effects on the on results of the proposed method. Patients age is particularly an important factor, because the water content in body depends on the age and health condition, which in turn affect the dielectric properties. Moreover, patient's weight can influence the SAR value. Finally, to better understand the applications and limitations of the proposed methods, it is necessary to perform lab experiments on human subjects, both with and without breast cancer. These experiments can help to better evaluate the advantages of proposed method over other current existing breast cancer detection technique.

REFERENCES

[1] Breast. `https://en.wikipedia.org/wiki/Breast`. Accessed: 2016-09-30.

[2] Tissue properties. `https://www.itis.ethz.ch`. Accessed: 2016-09-30.

[3] Bacon, L., W. Du, J. Ma, M. Petridis, and R. Lee (2010). *Software Engineering, Artificial Intelligence, Networking and Parallel/Distributed Computing 2010*, Volume 295. Springer.

[4] Barrett, A. H., P. C. Myers, and N. Sadowsky (1980). Microwave thermography in the detection of breast cancer. *American Journal of Roentgenology 134*(2), 365–368.

[5] Bowman, H. (1985). Estimation of tissue blood flow. *Heat transfer in medicine and biology 1*, 193–230.

[6] Byng, J. W., M. J. Yaffe, R. A. Jong, R. S. Shumak, G. A. Lockwood, D. L. Tritchler, and N. F. Boyd (1998). Analysis of mammographic density and breast cancer risk from digitized mammograms. *Radiographics 18*(6), 1587–1598.

[7] Foster, K. and J. Schepps (1981). Dielectric properties of tumor and normal tissues at radio through microwave frequencies. *The Journal of microwave power 16*(2), 107–119.

[8] Gabriel, C. (2005). Dielectric properties of biological tissue: variation with age. *Bioelectromagnetics 26*(S7), S12–S18.

[9] Gabriel, C., S. Gabriel, and E. Courhout. l996. the dielectric properties of biological tissues: I. literature survey. *Phys Med Biol 41*(223), l–2249.

[10] Greenstein, J. (1947). Biochemistry of cancer, new york acad.

[11] Homburger, F. and W. H. Flshman (1953). The physiopathology of cancer. new york, paulb. hoeber.

[12] IEEE Standards Coordinating Committee 28, o. N.-I. R. H. (1992). *IEEE Standard for Safety Levels with Respect to Human Exposure to Radio Frequency Electromagnetic Fields, 3kHz to 300 GHz*. Institute of Electrical and Electonics Engineers, Incorporated.

[13] Kopans, D. B. (2007). *Breast imaging*. Lippincott Williams & Wilkins.

[14] Kriege, M., C. T. Brekelmans, C. Boetes, P. E. Besnard, H. M. Zonderland, I. M. Obdeijn, R. A. Manoliu, T. Kok, H. Peterse, M. M. Tilanus-Linthorst, et al. (2004). Efficacy of mri and mammography for breast-cancer screening in women with a familial or genetic predisposition. *New England Journal of Medicine 351*(5), 427–437.

[15] Kruger, R. A., D. R. Reinecke, and G. A. Kruger (1999). Thermoacoustic computed tomography–technical considerations. *Medical physics 26*(9), 1832–1837.

[16] Lawson, R. N. and M. Chughtai (1963). Breast cancer and body temperature. *Canadian Medical Association Journal 88*(2), 68.

[17] Lee, C. H. and J. C. Weinreb (2004). The use of magnetic resonance imaging in breast cancer screening. *Journal of the American College of Radiology 1*(3), 176–182.

[18] Nass, S. J., I. C. Henderson, J. C. Lashof, et al. (2001). *Mammography and beyond: developing technologies for the early detection of breast cancer*. National Academies Press.

[19] NIHPublcation (2004). *Understanding breast changes*. Number 02-3536.

[20] Nilsson, S., S. Gustafsson, and L. Torell (1980). Skin temperature over a heat source: experimental studies and theoretical calculations. *Annals of the New York Academy of Sciences 335*(1), 416–428.

[21] on Non-Ionizing Radiation Protection, I. C. et al. (2010). Guidelines for limiting exposure to time-varying electric and magnetic fields (1 hz to 100 khz). *Health Physics 99*(6), 818–836.

[22] Pethig, R. (1987). Dielectric properties of body tissues. *Clinical Physics and Physiological Measurement 8*(4A), 5.

[23] Raaymakers, B., A. Kotte, J. Lagendijk, W. Minkowycz, E. Sparrow, and J. Abraham (2009). Discrete vasculature (diva) model simulating the thermal impact of individual blood vessels for in vivo heat transfer. *Advances in Numerical Heat Transfer 3*, 121–148.

[24] S. Rahmatinia, B. F. Magneto-thermal modeling of biological tissues: An step towards breast cancer detection. In *The 17th Biennial IEEE Conference on Electromagnetic Field Computation*.

[25] Schwan, H. P. (1971). Interaction of microwave and radio frequency radiation with biological systems. *IEEE Transactions on microwave theory and techniques 19*(2), 146–152.

[26] Valvano, J., J. Cochran, and K. Diller (1985). Thermal conductivity and diffusivity of biomaterials measured with self-heated thermistors. *International Journal of Thermophysics 6*(3), 301–311.

[27] Warner, E., D. B. Plewes, K. A. Hill, P. A. Causer, J. T. Zubovits, R. A. Jong, M. R. Cutrara, G. DeBoer, M. J. Yaffe, S. J. Messner, et al. (2004). Surveillance of brca1 and brca2 mutation carriers with magnetic resonance imaging, ultrasound, mammography, and clinical breast examination. *Jama 292*(11), 1317–1325.

VITA

Sepideh Rahmatinia was born on April 20, 1992 in Rasht, Iran. She received her Bachelor of Science in Electrical Engineering from Guilan University, Iran. She has submitted this thesis as a master student and research assistant at Renewable Energy and Vehicular Technology (REVT) laboratory at The University of Texas at Dallas (UTD). Her research interests include biomedical engineering, cancer detection, radio frequency application in biomedical engineering.